PAPER BASED INTEGRATED MICROFLUIDIC SYSTEM USING ELECTRO-OSMOTIC PUMPS WITH LIQUID BRIDGES

by

Ahmet Yasin Çelik

B.S., Electrical and Electronics Engineering, İstanbul Şehir University, 2016

Submitted to the Institute for Graduate Studies in
Science and Engineering in partial fulfillment of
the requirements for the degree of
Master of Science

Graduate Program in Electrical and Electronics Engineering
Boğaziçi University
2019

ACKNOWLEDGEMENTS

In my two-and-a-half years at Boğaziçi University, I was always with people who had an amazingly positive impact on me, both academically and personal vision. It is perhaps my greatest duty to give them my gratitude.

First of all, I would like to thank Professor Şenol Mutlu for giving me the opportunity of research with him and to his trust and encouraging. In this process, with his incredibly creative ideas presented to every problem I have encountered, it has helped tremendously in this thesis and other researches.

As for the BUMEMS Lab, I would like to thank Kemal who solved the existing problems very easily, Ozan with his always pleasant conversation and support, Gürkan who always shared his many experiences and Doruk who is one of the most enjoyable person to work with. Of course, I would like to thank Kerem for his creative ideas and discipline, which we have worked with during this process, where we have always exchanged ideas. Without him, it was almost impossible for this thesis to come here.

Finally, of course, I should not forget my family. It would have been impossible for me to come to this point if my dear wife Azra had not love and support at any moment in this process. She creates all the time Babylon on my mind and makes me more creative in my writing and research processes. If my dear grandfather Baki Çelik and his dreams were not encouraging me in my whole life, today I would not write this thesis. His vision and support was the basis of my determination and desire in this field. And lastly I would like to thank to my child Baki Mirza whom we were surprised to learn that he would join to our lives. He was my biggest source of energy to continue and come to an end of my master journey.

ABSTRACT

PAPER BASED INTEGRATED MICROFLUIDIC SYSTEM USING ELECTRO-OSMOTIC PUMPS WITH LIQUID BRIDGES

This thesis demonstrates a novel paper based microfluidic device with electro-osmotic pumping mechanism that was designed, optimized, simulated, fabricated and analyzed. Optimization of paper based electro-osmotic pumping was demonstrated for the first time using multi-physic finite element solver COMSOL, enabling 12 times better performance. Different fabrication methodologies were implemented, such as laser cutting, silicone melting, wax printing, and laser micromachining, providing easy, cost effective, and eco-firendly microfluidic chips. Results show that a 113 V/cm electric field creates a 50 μm/s electro-osmotic velocity with purified water and a 70 μA electrical current creates 1 μL/min volumetric flow rate with 2 mM NaCl solution in paper based channel. Moreover, continuous channel of paper based electro-osmotic pumps was implemented for the first time, where a 30 nL volumetric flow rate was created by 82 a V/cm electric field using 50 mM NaCl solution. Furthermore, electric field and volumetric fluid flow tests were done with solutions od different salinity. Hydraulic resistance was increased 57 times using papers with different porous structures. Finally, integration of paper based electro-osmotic pumps were demonstrated for the first time, including the paper based channel, motion control, continuous channel, mixing and metering units. Following the concludig remarks, necessary researches and experiments in order to improve control mechanism, understanding pH relations, integration of multiple pumping and wetting systems are discussed as a future work.

ÖZET

KAĞIT TABANLI ELEKTRO OSMOTİK POMPALARIN SIVI KÖPRÜLERİ İLE MİKROAKIŞKAN SİSTEMLERE TÜMLEŞTİRİLMESİ

Bu tezde, daha önce yapılmamış, kağıt tabanlı elektro osmotik pompaların sıvı köprüleri ile mikroakışkan sistemlere tümleştirilmesi anlatılmıştır. Sistem dizayn edilip, simülasyonlar yardımıyla en verimli hale getirilmiş, üretilmiş ve analiz edilmiştir. Optimizasyon işlemi alan içinde ilk defa COMSOL sonlu element çözüm programı ile yapılmış ve 12 kat daha iyi performans elde edilmiştir. Lazer ile kesme, silikon eritilmesi, balmumu çizimi ve lazer ile kanal açma gibi farklı üretim yöntemleri kolay, ucuz ve çevre dostu mikroakışkan çipler oluşturulmasını sağlamıştır. Saf su kullanılarak, 113 V/cm elektrik alan altında 50 μm/s elektrik osmotik akış elde edilmesi ve 70 μa elektrik akımı altında 1 L/dakika hacimsel sıvı akışı 2 mM tuzlu su ile elde edilmesi, tezin sonuçları arasında gösterilebilir. Ayrıca, sürekli kanal tümlemesi ilk defa yapılmış ve burada 50 mM tuzlu su kullanılarak, 30 nL hacimsel sıvı akışı, 82 V/cm elektrik alanı altında elde edilmiştir. Bununla birlikte farklı tuzluluk oranlarına sahip çözeltiler ile elektrik alan ve hacimsel sıvı akış deneyleri yapılmıştır. Kağıdın porlu yapısı esas alınarak, farklı por yapısındaki kağıtlar ile hidrolik direnç 57 kat artırılmıştır. Son olarak, kağıt bazlı kanal, hareket kontrolü, devam eden mikroakışkan kanal, ölçme ve karıştırma birimlerinin tümleştirilmesi gösterilmiştir. Gelecek çalışmalarda ise kontrol mekanizmasının arttırılması, pH ilişkisinin anlamlandırılması, çoklu pompa sistemlerinin anlaşılma ve uygulanması ile kağıdın ıslatılmasına ilişkin alanlarda araştırma ve deney yapılması planlanmıştır.

TABLE OF CONTENTS

LIST OF FIGURES

LIST OF TABLES

LIST OF SYMBOLS

CO_2	Carbon dioxide
E	Electric Field (V/m)
ec	Electric currents module
H_2O	Water
L_{pumping}	Length of pumping channel
Q_{bridge}	Volumetric flow in bridge channel
Q_{main}	Volumetric flow in main channel
Q_{pumping}	Volumetric flow in pumping channel
W_{bridge}	Width of bridges channel
W_{main}	Width of main channel
W_{pumping}	Width of pumping channel
ε	Permittivity of medium
ζ	Zeta potential
η	Viscosity
ρ	Resistivity
υ	Bulk liquid velocity

LIST OF ACRONYMS/ABBREVIATIONS

3D	Three-dimensional
ac	alternating current
CAD	Computer-aided design
dc	direct current
DI	Deionized (water)
DNA	Deoxyribonucleic acid
EDL	Electrical double layer
EOF	Electro-osmotic flow
EOP	Electro-osmotic pump
LOC	Lab-on-chip
MEMS	Micro-electro-mechanical systems
PMMA	Poly(methyl methacrylate)
br	Brinkman equations module
spf	Laminar flow module
tds	Transport of diluted species module

1. INTRODUCTION

Lab-on-chip (LOC) devices were originally designed to be used in order to solve problems of analysis and synthesis of samples in small quantities. Miniaturization of chemical and biochemical analysis systems extends the capability of devices, decreases the time consumption and the cost thanks to high throughput processing and analysis methods [2]. "Microcircuits of the fluidic work" would be employed to manipulate small volumes of samples. Main advantages of this approach include low requirements for expensive space, reagents, and waste, reducing cost and time [3]. These devices have the potential of replacing large laboratories in the future, in effect, reducing the number of required personnel and enabling the access to performed services even in rural areas. They can be applied in many areas such as pharmaceutical, medical, and food industries, biological and chemical analysis, environmental sensors and printers and they show great potential. On the other hand, for the time being, due to the problems such as the cost of production and the non standardization, microfluidic devices cannot be widely commercialized but can only be integrated into existing systems. As a result the field is still open for the development of more practical solutions.

One of the most common research topics in LOC field is paper based microfluidic devices. Paper based microfluidic devices are a recent class of microfluidic systems that generate high-technology function from a low-technology material [4]. Paper based applications are commonly used in electro-osmosis, electrophoresis, and electrokinetic tools. Electrokinetic phenomena, in conjunction with the capillary and viscous effects, plays a significant role in progressively enhancing the liquid flow rate through the paper channel with increasing magnitude of the applied electrical potential [5].

1.1. Potential of Electro-Osmotic Pumping

As previously discussed, paper based microfluidic devices have great potential, especially in LOC environments. Electro-osmotic pumps (EOPs) play an important

role in this domain, because they provide integration abilities. A clear advantage of field-induced pumps over membrane pumps is that they do not require moving parts, such as check valves, which complicate the fabrication, sealing, and operation of these systems [6]. Porous media enables elimination of pressure driven or back flow, making systems are more reliable. In a porous medium completely closed to external flow, the electro-osmotic and induced pressure-driven flows combine to yield zero net flow and maximum electro-osmotic pressure. Electro-osmotic permeability, or the resistance to electro-osmotic flow (EOF), is independent of the pore size [7].

In general, the approach described above involves a large number of porous dielectric materials, porous membranes or microparticles packed in the pumping microchannels, forming electro-osmotic sub-microchannels or nanochannels. By applying operation voltage on the porous media, the EOFs in the porous media can provide very high pumping pressures and sometimes high-rate flows [8]. It can be clearly seen that creation of high and low pressure is beneficial in LOC environment and as research show us EOP has great potential in this domain.

1.2. Motivation and Novelty

Motivation of this thesis is to explain the working principle of a practical, cost effective, and integratable EOP on paper with liquid bridges. The said EOP was designed, optimized, implemented, and finally integrated with the rest of the system. These pumps and channels would be the building blocks of a paper-based integrated microfluidic system designed for mixing and metering. EOPs are attractive for integrated microfluidic systems using polar liquids since they have no moving parts and can be easily integrated. However, the pump's hydrodynamic resistance is low for channels with hydraulic diameters greater than 1 μm, hence the results in back flow and low pressure gradients. Porous plugs, in this case paper substrates, offer a promising solution by both increasing the resistance to pressure-driven flow and the surface area of the pump [9]. However, if the electrodes are placed at the ends of the channel, the required bias voltage is very high (greater than 500 V), and the electric field extends along the entire channel. If they are located immediately up-stream and

down-stream of the porous plug within the channel, the voltage is reduced (less than 50 V), but air-bubble evolution blocks the flow [9]. Instead, an electrically conductive liquid connection through a high impedance (i.e., low-flow) porous plug branch can be used so that bubble generating electrodes are placed on the reservoirs where generated bubbles can escape to air without interfering with liquid flow [10]. Liquid electrodes, gel or salt bridges have been used for this purpose before [10,11]. In this thesis, for the first time, optimization and integration steps were performed in this regard. Moreover, handmade fabrication process plays an crucial role in this thesis.

1.3. Outline of the Thesis

Up to this point in Chapter 1, information from historical perspective to today's world is described. Moreover, previous works and research was analyzed and motivation and novelty were demonstrated.

In Chapter 2, the concepts of EOPs will be demonstrated and principle of operation will be described. Moreover, optimization process will be shown with using COMSOL multiphysic, and then device parameters and operation principles will be explained.

In Chapter 3, fabrication process will be described. Three main methods used in fabrication are laser cutting, hot melting silicone, wax printing and laser micromachining process that enable the simple, cost effective, and fast fabrication of microchips.

In Chapter 4, measurement devices and methodologies will be mentioned. Moreover, paper based channel, continuous channel and their integration will be shown.

In Chapter 5, concluding remarks will be made, and future work plan will also be given.

2. THEORY AND SYSTEM DESCRIPTION

2.1. Theory of Electro-Osmotic Pumping Mechanism

EOF has been a well-used phenomenon since the 19th century, where it has been utilized to pump water from soil [12]. However, application of EOF in the field of microfluidics is relatively new. In micro total analysis systems, EOPs are used for precise liquid manipulation both under alternating current (ac) and direct current (dc) voltages [13]. However, since high electric fields result in electrochemical reactions in faradaic regions, gas formation occurs due to electrolysis of water, clogging microchannels. To overcome that, liquid bridge mechanisms with porous materials were developed on EOPs, which are called porous plugs, as seen in Figure 2.3 [12]. By implementing liquid bridge connections, effect of gas formation is eliminated. A comparison of laminar flow with EOF shows that laminar or pressure driven flow does not yield bulk movement, on the other hand, as following chapters also demonstrate, EOF constitutes bulk flow.

Paper based chips have porous structures that provide lots of opportunities for EOF,such as lower back pressure flow. In equation 2.1, υ, ε, ζ, E, η refer to bulk liquid velocity, permitivity of medium, zeta potential, electric field along the channel, and viscosity, respectively. As the formula describes, bulk liquid velocity can be positively affected with changing permitivity, electric field and zeta potential.

$$\vec{\upsilon} = \frac{\varepsilon \zeta \vec{E}}{\eta} \tag{2.1}$$

2.1.1. Principle of Operation

The charged surface attracts counter ions and repels co-ions in the solution. Deportation usually leaves the solid surface negatively charged, causing the surface to attract positive ions in the solution. A double layer of ions is formed, consisting of a compact immobile layer and a mobile diffuse layer in the liquid [10]. If an electric field is applied parallel to the interface, mobile charges in the diffuse layer are moved, (dragging the liquid with them) while charges in the compact layer remain immobile as seen in Figure 2.2. This movement of liquid as a result of the electric field is the EOF [10]. In this manner, electric field plays an important role in operation, so all experiments were done measuring electric current to make sure system has electric field. Moreover, all designs were simulated in the light of this approach.

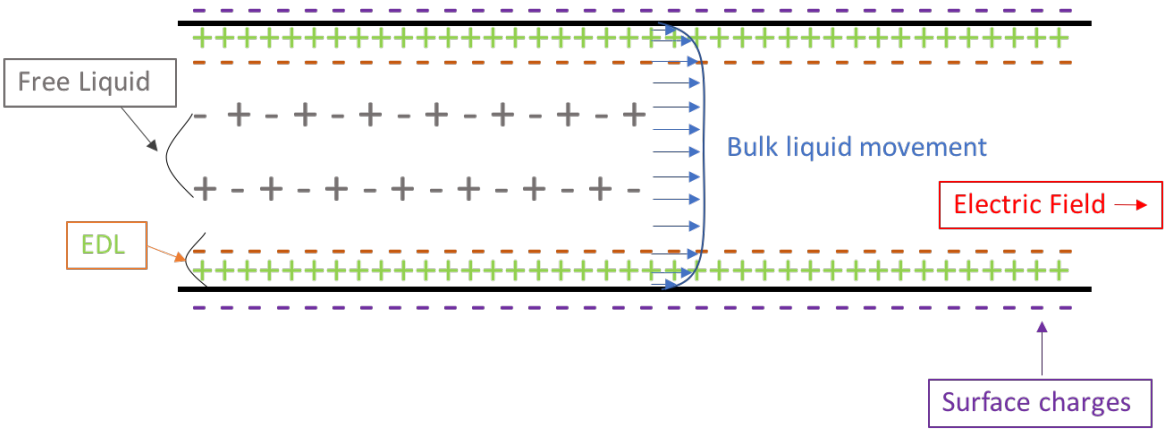

Figure 2.1. Demonstration of bulk liquid velocity profile of EOF flow.

EOPs are suitable for microfluidic applications because they can be made very compact and deliver high pressures. Moreover, they can produce a pulse-free flow without incorporating any moving parts. In EOPs an electrolyte is pumped by applying an electric field to the charged Debye layer [14]. When a polar liquid (such as water) and a solid (such as glass) come into contact, the solid surface acquires an electric charge, which influences the charge distribution within the liquid and causes a 2-layer charge distribution called the electric double layer or EDL. The charges close to the wall are strongly drawn toward the surface, but the application of an electric field can change

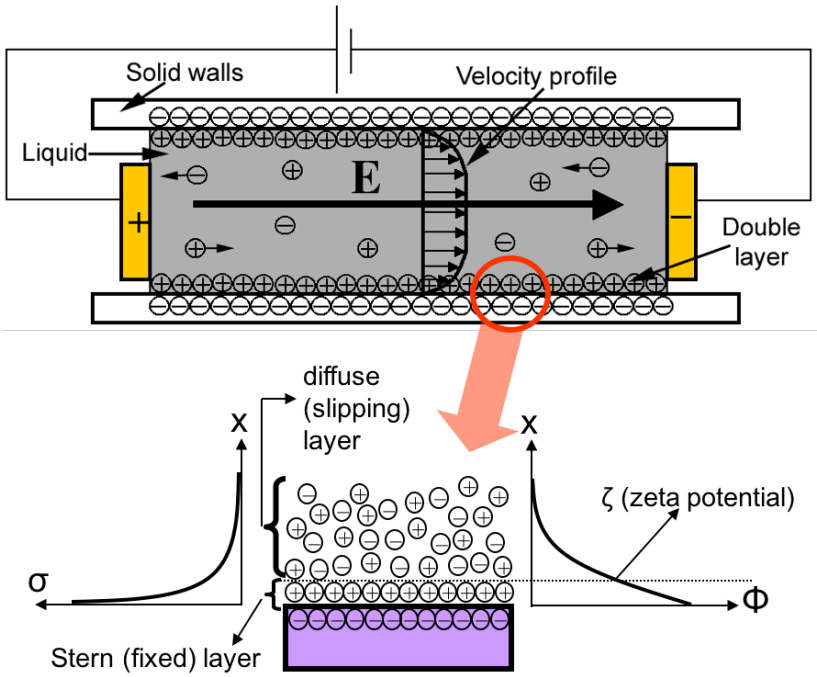

Figure 2.2. Theory of electrical double layer, Zeta potential of EOF [10].

the charge distribution deeper in the fluid [15]. Paper based electro-osmotic pumping mechanism has no moving parts and the porous structure is able to create EDL easily. Figure 2.2 shpws that EDL has two components which are stern (fixed) layer and zeta potential, respectively. These two components include diffuse (slipping) layer that is directly affected by the applied electric field.

2.2. Device Description

The parameters of the device are shown in Figure 2.4. The voltage difference on the reservoirs of the bridge sections creates an electric field and an electrical current, across bridges, in the pumping channel of the device while creating circular field lines towards the field-free regions (main channel region). The undesired fluid flow in the bridge sections is labelled as Q_{bridge} and the desired flow rate in the field-free region as Q_{main}. As the figure describes, there are two electrode reservoirs in the system where voltage is applied to create the electric field in the system. As Q_{main} shows, two places can be defined as inlet and outlet regions, which can also be called field free

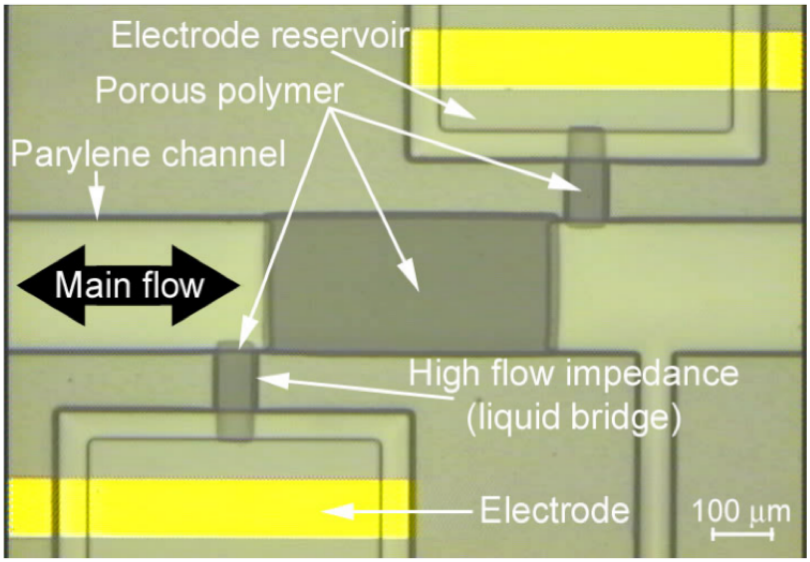

Figure 2.3. Porous-plug EOP with liquid bridges using porous polymer and parylene microfluidic channels [10].

regions. There are two bridges where minimum fluid flow is created and for which the L pumping is the destination.

2.2.1. Modeling of Paper Based EOP

The electro-osmotic micropumps generate an EOF of electrolytes. Charged electrodes cause the electrolyte polarization, which results in the formation of clouds of ions, the electric double layers, above the electrodes. Component of the electric field, which is tangential to the channel walls, than accelerates the ions along the surface and the electrolyte bulk is dragged by viscous forces [16]. Paper based structure enable to porous structure, in this manner, it could be said that creation of EDL in porous structure can also work. Moreover, some papers can be hydrophobic, even they are, they are still very useful materials in EOP. Hydrophilic and hydrophobic surfaces, accurate prediction of the electrokinetic potential depends on the veracity of models for both (i) interfacial charge formation, and (ii) diffuse and condensed ion distributions [17].

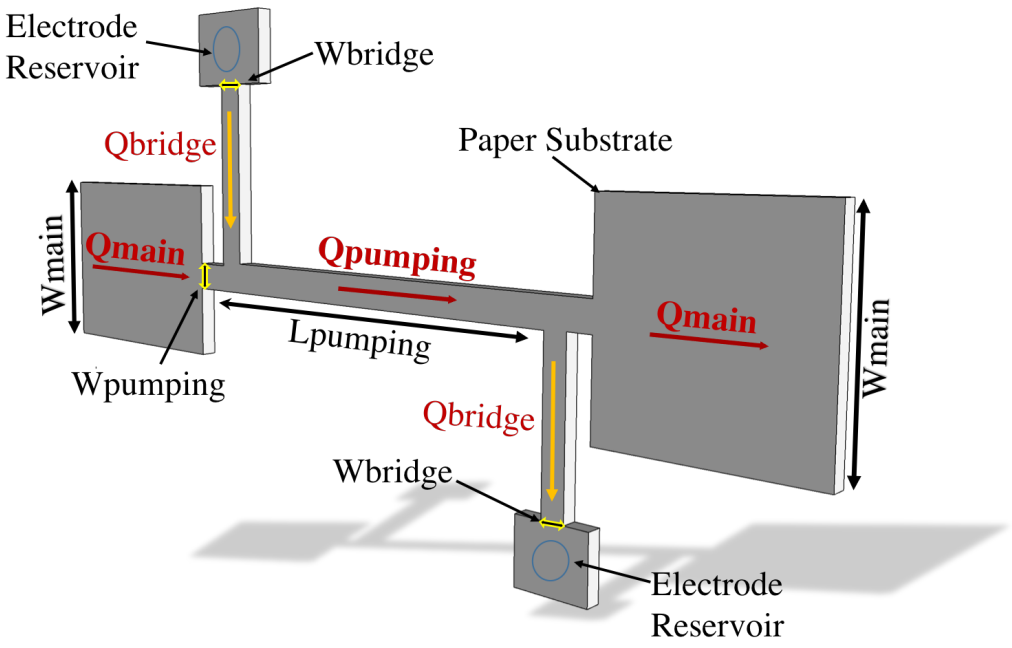

Figure 2.4. Demonstration of device parameters of paper-based EOP.

2.3. Device Simulation

To understand EOF in porous media, multi-physics should be implemented in finite element simulation. Simulation is the basis of the determination of device parameters, so that the volumetric flow approaches at its maximum value, without creating back flow. In this part of the thesis, how simulation play a crucial role for optimization process will be shown.

The main purpose of the simulation is analyzing better design alternatives, reaching convenient parameters and understanding proper physics elements in the research. In order to achieve this, four modules (spf, ec, br, and tds, representing laminar flow, electric current, Brinkman equations and transport of diluted species) were created and simulated in COMSOL 5.2. In this manner, basis of design implementation shows us Q_{main}, Q_{bridge} and Q_{pump} parameters, which stand for net flow in main channel, net flow in bridge channel, and net flow in pump channel, respectively. They are basically related to the spf. Moreover, when it comes to electric fields streamline, ec provides

valuable information regarding the magnitude of electric field, direction of electric field, and the electric potential. Furthermore, paper substrate has unique porous structure which is represented via Brinkman equations with size properties. Last but not least, change in concentration can be a key phenomenon to understand simulation accuracy and proper operation which is accounted for by the tds. Following this approach, spf was integrated into the system to be able to analyze the flow rate and direction in the system. Figure 2.5 describes velocity field in time as a, b, c, and d, with respect to t1, t2, t3, and t4. As a result of this simulation provides accurate approach for design.

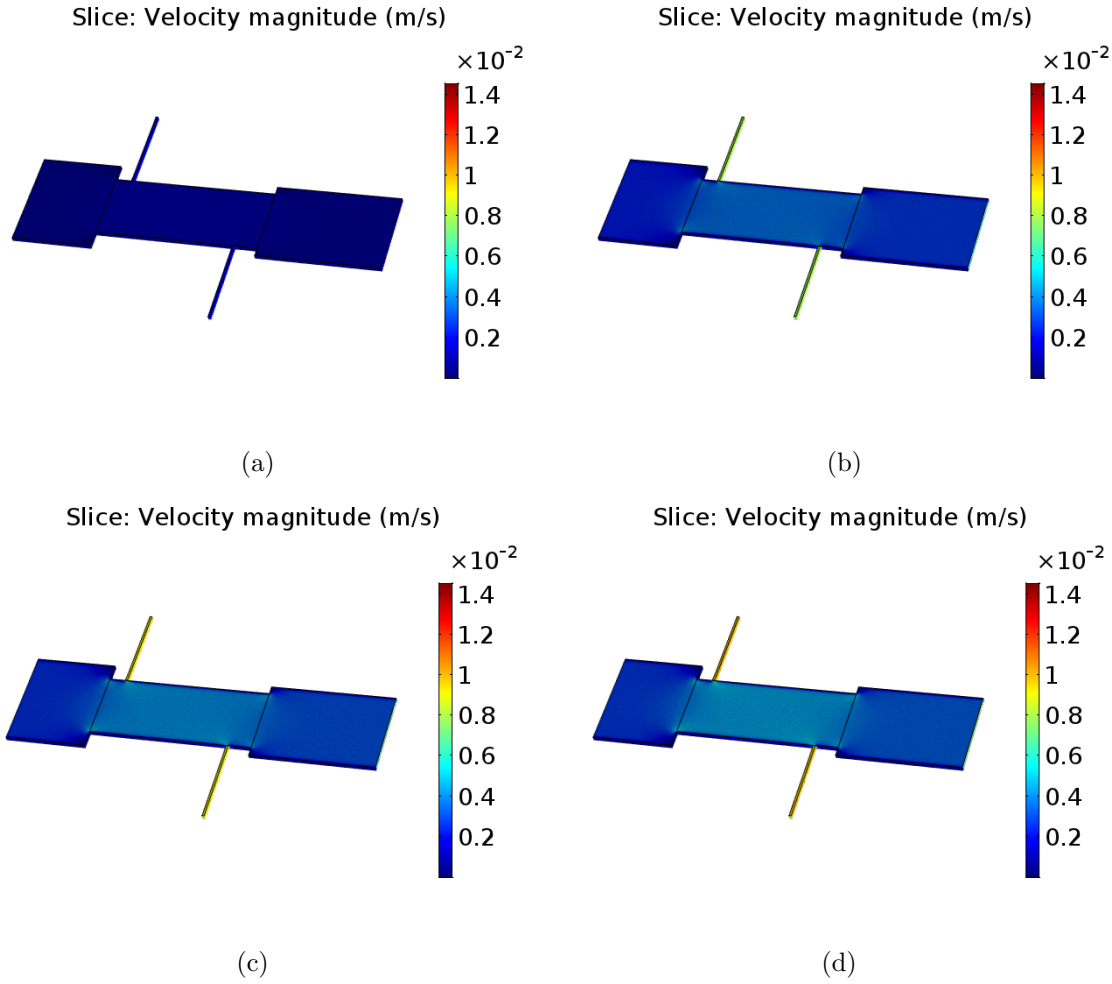

Figure 2.5. Modeling Comsol Simulation with velocity field with result of multiphysic. (a),(b),(c) and (d) show time step of simulation t=0, t=1, t=2 and t=3 respectively

At the fundamental microscale the Stokes equations apply and provide a complete description of the entire flow field. However, as a result of the complex and often only statistically known geometry of the solid surfaces in the medium, solution of the Stokes equations is generally very difficult. On the macroscopic level, Darcy's law, first established empirically but more recently derived formally by performing appropriate volume averages of the Stokes equations, is applicable [18]. Brinkman equation provides porosity and analyzing low flow rate in the system which is eliminated from external pressure such as atmospheric and internal pressure. By doing that, we have more accurate results while analyzing EOF. Electric current module enable to us create electric field in two gates where we are able to see electric field stream line that plays crucial role to start flow in the paper substrate and free channel. Before achieving the results, we define inlet and outlet of the system with Laminar flow module that is connected with Brinkman Equations and Laminar Flow module as multi-physics where finite elements measurement were done.

2.4. Device Optimization and Parameters

Optimization process is based on achieving a maximum Q_{pump} as previously discussed. Parametric sweep of increasing internal hydraulic resistance is one useful tool to achieve this. By doing so, load channel can be linked to the system with the best pump performance. Comsol simulations show that the length of the pumping channel L_{pumping} has direct proportion and the width of the pumping channel W_{pumping} has inverse proportion with respect to the volumetric flow. It is an undeniable fact that achieving accurate volumetric flow requires the minimization of the flow rate of the bridges. That is why their size should be as low as possible. Following this approach, simulation process is expected to represent the real life limitations so that it provides more definitive data regarding the fabrication of devices. For the parametric sweep, all parameters except for W_{main} were fixed at the first step. Results show that W_{main} should be maximum within fabrication limitations in order to reach best pumping flow rate. Secondly, all variables were fixed to find the most lowest W_{bridge} size within fabrication limitations. Third parameter to sweep for was L_{pumping}. Its size should

be long to achieve again maximum Q_{main} ratio with respect to Q_{bridge} while all other parametric variables are fixed. Last but not least, it was observed that W_{pumping} has a parabolic trend with other parametric variables achieving reasonable and accurate flow rate in pumping area. As a result, an optimized pump design with parameter ratios of 1:80:20:70 for W_{bridge}, L_{pumping}, W_{pumping} and W_{main}, respectively, to achieve maximum flow rate was determined [19].

Theory behind of EOP is also shown in simulation. In order to achieve maximum Q_{pump} the back flow and Q_{bridge} should be minimized. In Figure 2.6, blue stream line shows the electric field that generates EOF in field free region. Red streamlines demonstrate that EOF will be observed mostly in field free region, and it is rarely seen in the bridge side. Also, as it will be observed later in experimental study of pH measurements, simulations clearly established movement of fluid in field free region. Lastly, Figure 2.7 shows the simulated pressure contours on the same system.

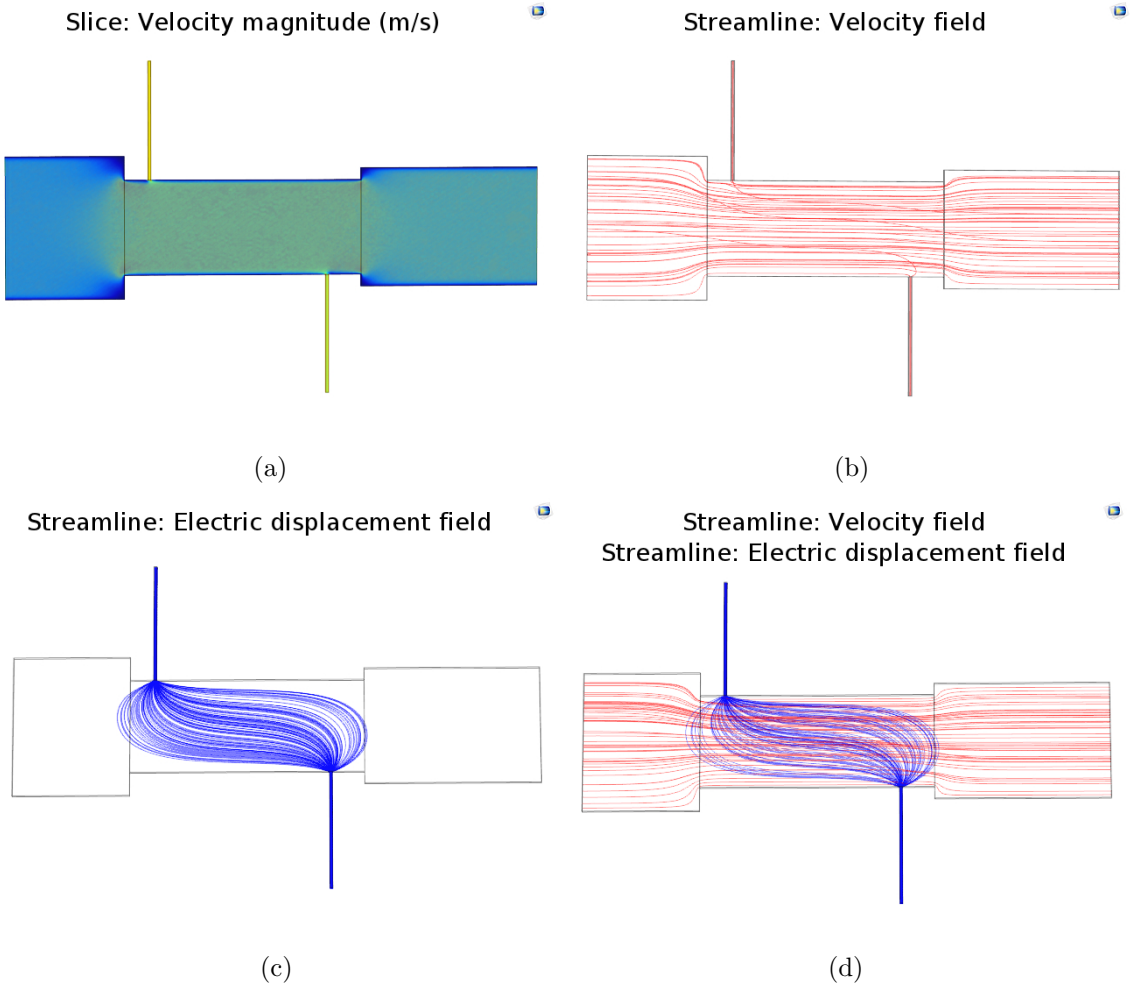

Figure 2.6. Modeling Comsol Simulation. (a) shows velocity demonstration, (b) velocity field streamline demonstration, (c) electric displacement field streamline with filter, (d) combination of electric field streamline and velocity field streamline

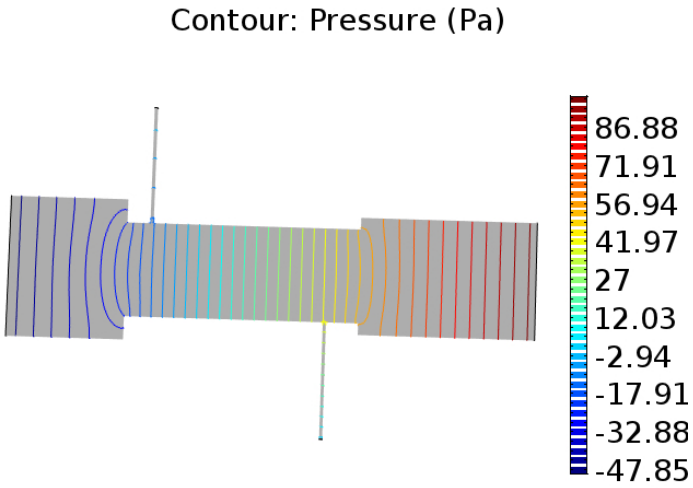

Figure 2.7. Demonstration of Pressure Simulation.

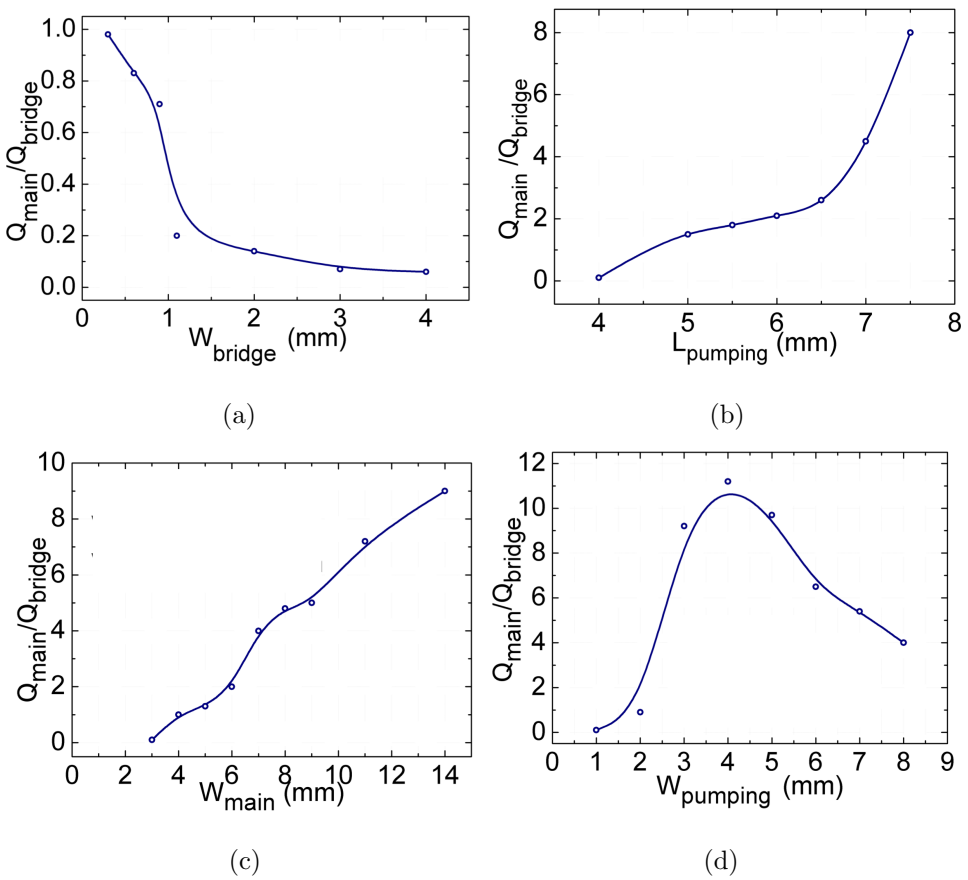

Figure 2.8. Computational optimization of Qmain/Qbridge based on the device parameters; a) Wbridge b) Lpumping c) Wpumping d) Wmain [19].

3. STRUCTURE OF THE FABRICATED DEVICE

3.1. Fabrication

In this chapter, two different fabrication methodologies will be discussed. Fabrication methodologies are based on simulation results. It was noted that hot melt silicone methodology could not be the most efficient way to build a EOP microfluidic chip. In related section, the crucial obstacle will be discussed. Secondly, wax printing methodology will be discussed that provides lots of opportunities and conveniences. All fabrication methods are based on three different papers types which are shown in in Figure 3.1. The three different approaches have different requirements for the fabrication process. To understand this requirement, Table 3.2 clearly show us ISO-Lab Cellulose Acetate and Iso-Lab Nitrocellulose have different properties with respect to thickness, pore percentage and pore size compared to Whatman Grade paper. Furthermore, it is seen that cellulose acetate can act hydrophobic, when it is not clean.

(a) (b) (c)

Figure 3.1. a)Side view of Iso-Lab 0.2 μ CA Membrane Filter, b)Side view of Iso-Lab 0.2 μ Nitrate Membrane Filter, c)Side view of Iso-Lab 10 μ Whatman Grade

3.1.1. Laser Cutting Process and Hot Melt Silicone Method

The hot melt adhesive wax can realize bridge bonding between various materials, such as paper, poly(methyl methacrylate) (PMMA) film, sheet glass, or metal plate.

Table 3.1. Comparison of Whatman Chromatography Number 1, Cellulose Acetate and Nitrocellulose papers with respect to average pore size, pore percentage and thickness.

	Whatman Grade 1	Cellulose Acetate	Nitrocellulose
Average pore size (μ)	10	0.2	0.2
Pore percentage (%)	70	70	70
Thickness (μ)	0.2	0.12	0.12

The bonding process is reversible and the wax is reusable through a melting and cooling process [20]. As described in previous works, laser cutting also plays an important role. Laser cut quality cannot be easily predicted. This is due to the dynamic nature of the laser cutting process, and it is particularly obvious when cutting ferrous alloys using oxygen as an assisting gas. The oxidation reactions with iron and other alloying elements add another source of heat and material removal occurs at two moving and often interacting fronts, the oxidation front and the laser beam front [21]. It can be seen that with laser cutting process, it is possible form microfluidic structures by cutting papers and creating channel on the poly-carbonate plate. It is important to note that, cutting paper with laser is a very delicate process that would be related to power and speed units in laser machine.

Fabrication process is shown in Figure 3.3. In this fabrication methodology, both sides of the cut paper are coated with hot melt silicone and covered with transparent laminating sheets. The stacked films are pressed in a thermal laminator with a roller system to achieve a uniform, flat and transparent structure. Finally, the holes are drilled on the reservoir regions. Laser cut and laminated samples are fabricated in different thicknesses. So, experimental results obtained from laser cut samples were very few due to poor performance of the chips, defects on paper and clogging pores by hot melt silicone. In Figure 3.4, we see time-lapse microscope images of the one of the few working samples. At t=0, experiment started with 500 difference in order to

move liquid from Main Channel 1 to 2, at t=270s concurrent motion towards Main Channel 2 over A and B regions was observed. From t=270 s onward, voltage polarity was reversed and at t=540 s reverse concurrent motion towards Main Channel 1 was observed. But this methodology has the wetting problem, which could block creation the electric field in the channel. The wetting process time was noted to be one or two hours.

Table 3.2. Channel parameters of CO2 laser cut. The parameter of "p" refers to power of laser machine and "s" refers to speed of laser machine.

	Line (μm)	Engrave (μm)	Width(μm)	Engrave (μm)
p10 s10	123.7	203.5	366.45	386.76
p20 s10	308.5	582.7	267.6	478.46
p30 s10	386.2	950	296.15	535.84

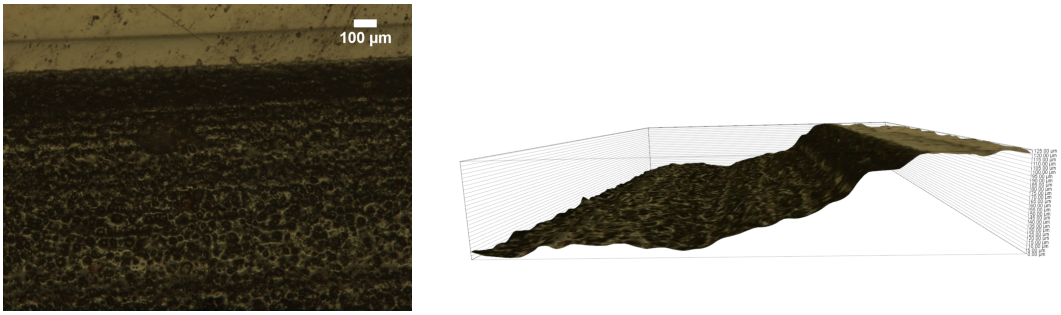

(a) (b)

Figure 3.2. Demonstration of measurement of laser micromachining channel. (a) Photograph of channel; (b) 3D reconstruction of the side view channel profile.

3.1.2. Wax Printing Method

Patterning paper with wax is a new technique for the microfluidic applications. Desired boundaries are printed with solid ink wax printers and printed paper samples are put on a hot plate [22]. However, solid ink wax printers are losing their relevance nowadays. Since we did not have one of solid ink wax printer, a custom plotting tool

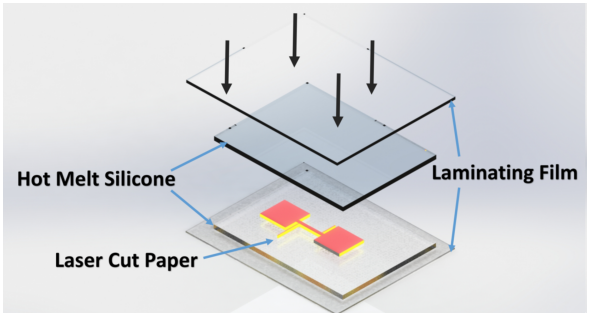

(a)

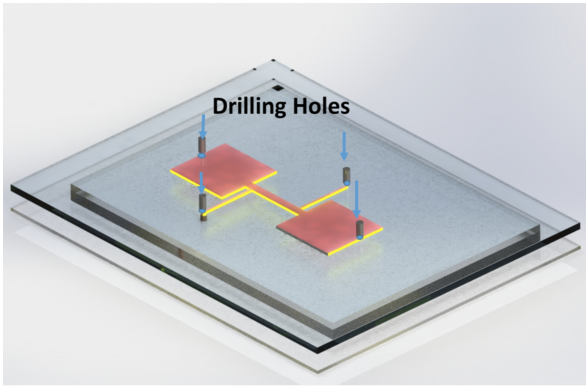

(b)

Figure 3.3. Fabrication process steps of the device. (a) Both sides of the cut paper are coated with hot-melt silicone and covered with transparent laminating sheets. The stacked films are pressed in a thermal laminator with a roller system to achieve a uniform, flat and transparent structure. (b) The holes are drilled on the reservoir regions.

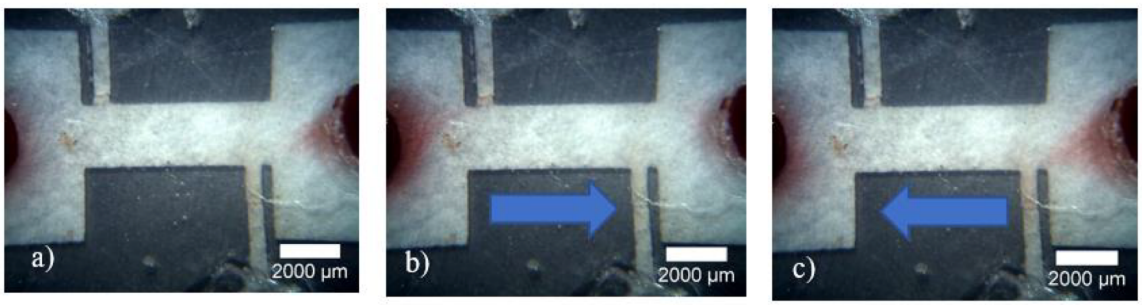

Figure 3.4. An example of fabricated chip with laser cut and hot melt silicon

was made. A 3D printer heater and a 0.3 mM nozzle is attached to the CNC machine to get precisely controlled wax printing pen and and its capabilities as seen in Figure 3.6. The process for patterning paper with wax is very simple, which can either be done at home using a wax pen or massively produced with a wax printer [23]. Previously, a hand made wax pen was created with voltage control, but it did not have a performance reliable enough to create straight features because of nozzle. Nevertheless, it can be considered as an alternative when 3D printer is not available. Moreover, having the ability to make corrections on the paper can be beneficial in some situations. Compression analogy is similar to writing a pen versus printer. Wax printer system is based on creation of an electric current to heat up the thermal heater, while CNC machine is connected to a computer that controls movement in x,y, and z directions. In this way, we can realize an automated wax printer system as shown in Figure 3.7.

Controlling the heater voltage and lateral speed of the CNC router, wax thickness can be adjusted to have a minimum channel width as 0.4 mm. It is based on voltage and current read by the multimeter, the resistance of the nozzle remains same in the drawing process. However sometimes different voltages can be applied depending on the shape and features. Thickness of wax on the paper is directly proportional with voltage. However, it can be emphasized that after 95 V, wax can not be written on the paper. If enough wax is present, consistent multiple samples can be printed easily in one printing session. Duration of one paper drawing is about 3 minutes.

After shaping wax layer on the paper, poly-carbonate plate should be prepared. In this process, laser micro-machining was applied for creation of reservoir holes for the gates and screws. In this process, the design was created layer by layer in CAD environment so that the gates and electrode reservoirs fit precisely to paper substrate. After that, adhesive film was integrated on the poly-carbonate plate to prevent leakage, and formation of gaps and changes in atmospheric pressure. Wax printed paper samples are sandwiched by poly-carbonate plates using adhesive tapes. An assembly schematic of paper based EOP with liquid bridges is shown in Figure 3.8. Actual device can be seen in Figure 3.9.

Last but not least, another fabrication methodology can be seen in Figure 3.8. This fabrication method enables the creation of continuous microfluidic channels where the flow can be controlled via EOP. In this process, similar to paper based fabrication, custom made wax printer draws the border of the channel. Melting point of paraffin wax is 58°, which was satisfied by the resistance of the nozzle that is fed from voltage source. When the paper is ready for experimentation, it is attached to the bottom of PMMA plate. Another PMMA plate is engraved by the laser machine to realize the continuous microfluidic channel. In the meanwhile, reservoir holes are created by the laser cutting method. Finally, plates are secured tightly by nuts and bolts. Carbon electrodes, which eliminate bubble and heat resistance significantly, and cables are attached to reservoirs. Finalized devices can be seen in Figure 3.10.

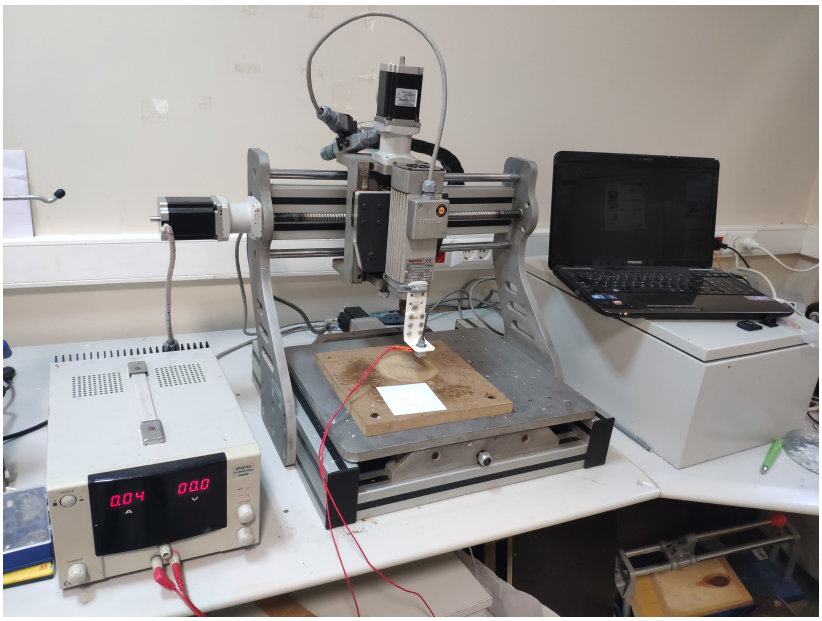

Figure 3.5. Photograph of the wax printer system.

3.1.3. Laser Micromachining

For a particular micromachining application the choice of laser is now judged as much by criteria such as process speed, part throughput, reliability, service intervals, capital, and operating costs of the overall machine tool rather than solely by the quality of the processed part [24]. Laser methodology is optimized and analyzed in

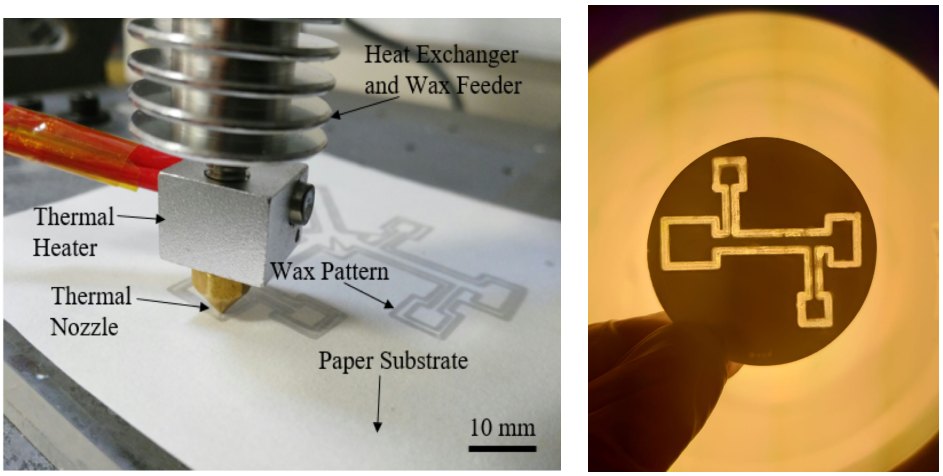

(a) (b)

Figure 3.6. Photograph of wax printing step (a) and (b) fabricated device. [19]

Table 3.2. In this table, "p" refers to power of the laser machine and "s" refers to speed of the laser machine. Table 3.2 shows us that increasing power creates higher depth in the poly-carbonate plate. On the other hand, speed has inverse proportion in for the depth of engraved feature in poly-carbonate plate. Figure **??** shows channel depth where the analysis was done via microscopic measurement.

There is a number of poly-carbonate plates that allow laser micromachining process. The PMMA material is a non-porous solid in room temperature and therefore contamination caused by bio-molecule adsorption is diminished. In addition, PMMA is inert in neutral aqueous solutions and no hydrolysis occurs during operation [25]. Paper substrates are needed to be precisely cut according to optimum design parameters. VersaLaser 30 W CO_2 laser is used with 10 % power and 30 % speed settings to cut features on the Whatman Grade 1 CHR paper. Hot melt silicone is applied to the paper substrate and sample is laminated. Reservoir holes are drilled on the sample. An example is presented in Figure 3.12.

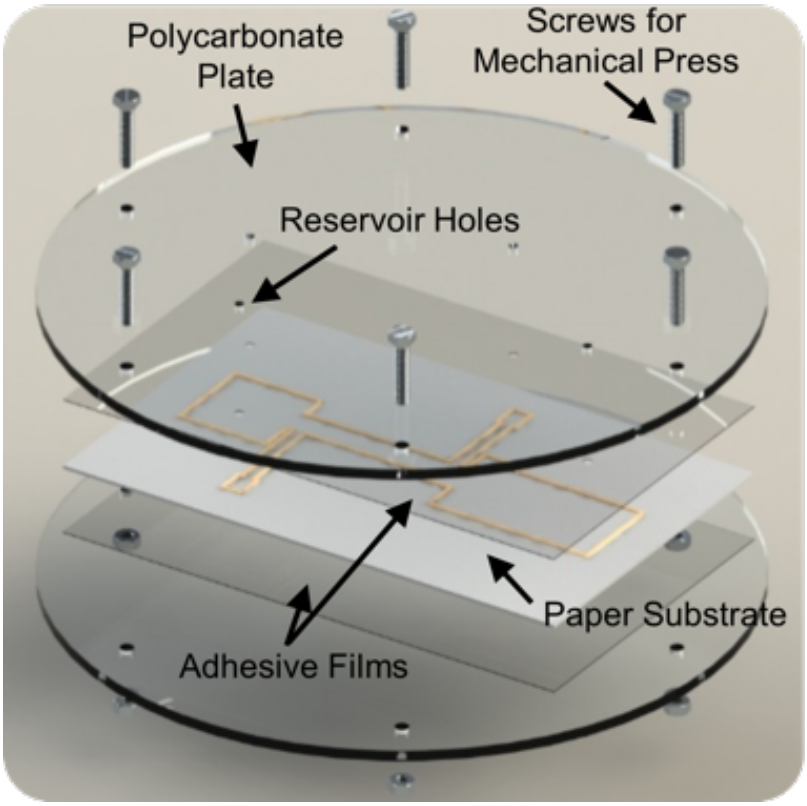

Figure 3.7. Fabrication process steps of the device: Wax thermal nozzle connected to a 3 axis CNC router to draw borders of design on chromatography paper. Adhesive films and polycarbonate plates press the paper substrate on both sides. Drilled holes act as reservoir openings [19].

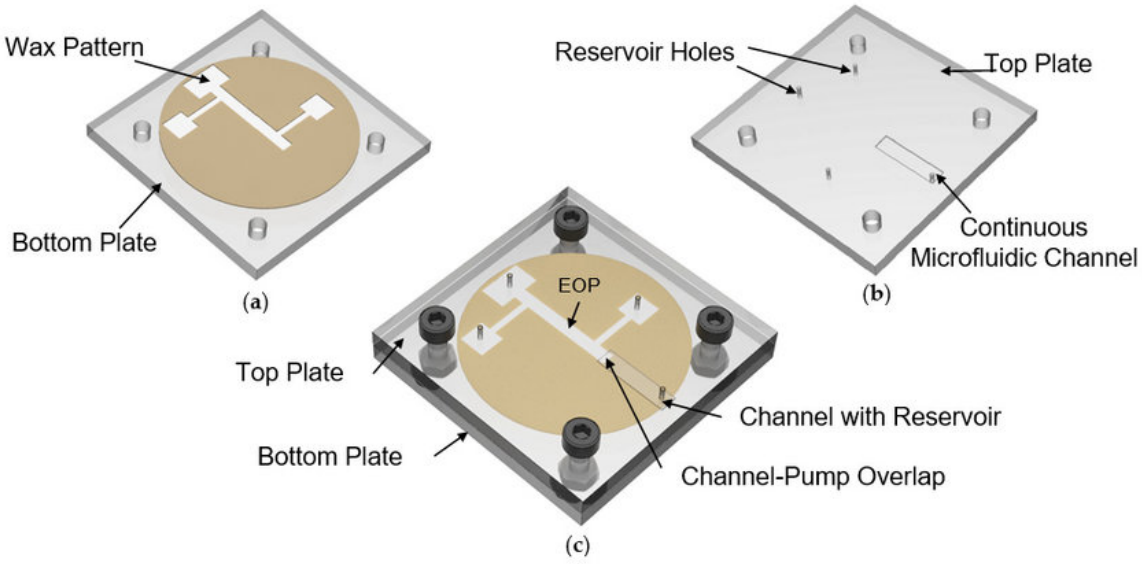

(a)

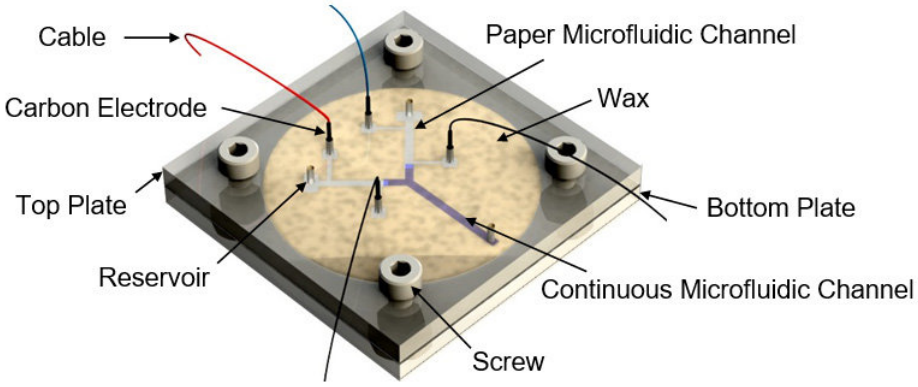

(b)

Figure 3.8. Demonstration of fabrication steps and fabricated device in bottom. Fabrication of the system in top :(a) Wax pattern is extruded on paper. Paper is held on the bottom plate;(b) A continuous microfluidic channel and reservoir holes are made on top plate using a laser cutter; (c) Top plate is placed upside down on bottom plate and mechanically secured after wetting plate surfaces. [1]

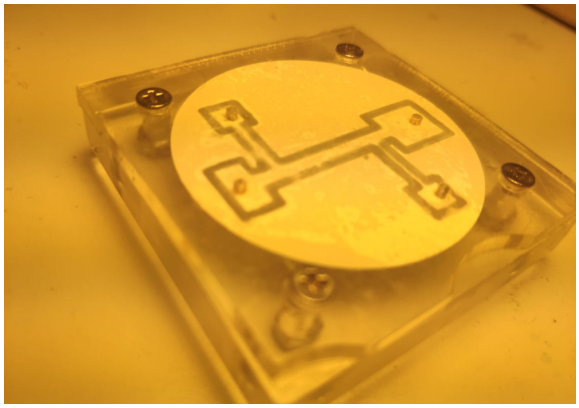

(a)

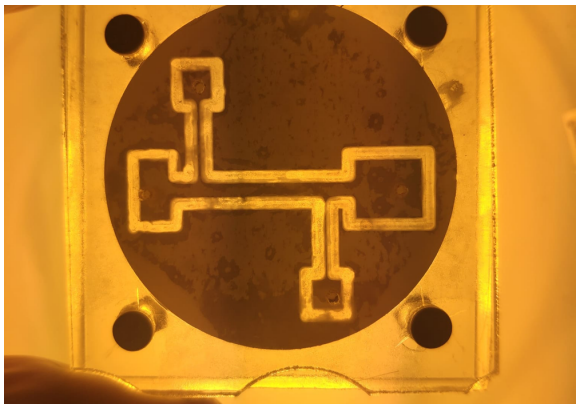

(b)

Figure 3.9. Photograph of the paper based microfluidic device.

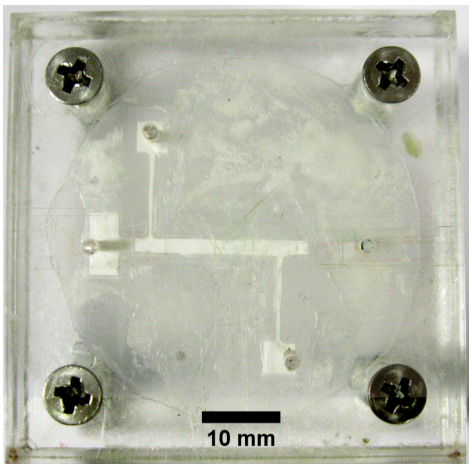

Figure 3.10. Photographs of the continuous microfluidic device.

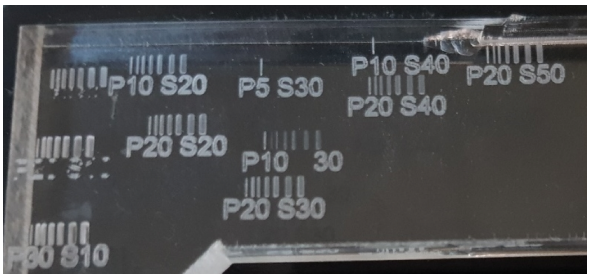

Figure 3.11. Demonstration of channel parameters of CO2 laser cut.

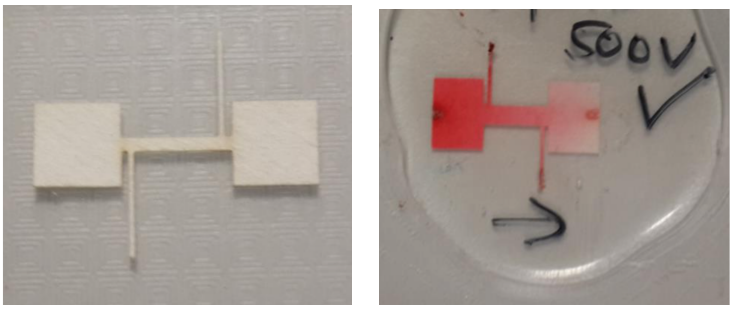

(a) (b)

Figure 3.12. A laser cut paper substrate with 0.3 mM bridge width and a laminated sample with hot melt silicone

4. CHARACTERIZATION MEASUREMENTS AND RESULTS

4.1. Measurement Equipment

Flow experiments are done with different dc voltages from -500 to 500 using Keithley 487 Picoammeter/Voltage Source. DC current is read with an ammeter. Carbon electrodes are used instead of metal ones to minimize electrochemical reactions. Food coloring is added to differentiate flow. A light microscope with Motic Moticam 1000 attached is used to analyze the speed of the dyed water. A photograph of the setup and voltage source is shown in Figure 4.1. It can be clearly seen that two dc voltage sources can be used based on the number of EOPs. Ammeter and voltmeter enable to analyze electric current and voltage that demonstrates the presence of the electric field in microfluidic chip. All measurements and image analyses were done in ImageJ which is also know as. ImageJ basically peforms segmentation operation by selecting the same color pixels searching the neighboring pixels around them. ImageJ is macro compatible, enabling the writing of small macros to calculate area differences of these measurements [26]. All data are based on sequence photos or videos of experiments that were analyzed via pixels methodology that provides volumetric flow rate of our system. In depth of microfluidic and laser micromachining were analyzed in Figure 4.2. Moreover, test environment is shown in Figure 4.1.

4.2. Pressure Driven Flow

Pressure driven flow is one of the most important phenomena, because back flow and pressure driven flow should be prevented to achieve more accurate results in experiments. Moreover, it is an undeniable fact that measurement results are affected by pressure driven flow whether the impact is positive or negative. Even though porous materials eliminate the pressure driven flow, measurements should be done to observe the total impact on the system. Moreover, this calculation provides us an aspect to

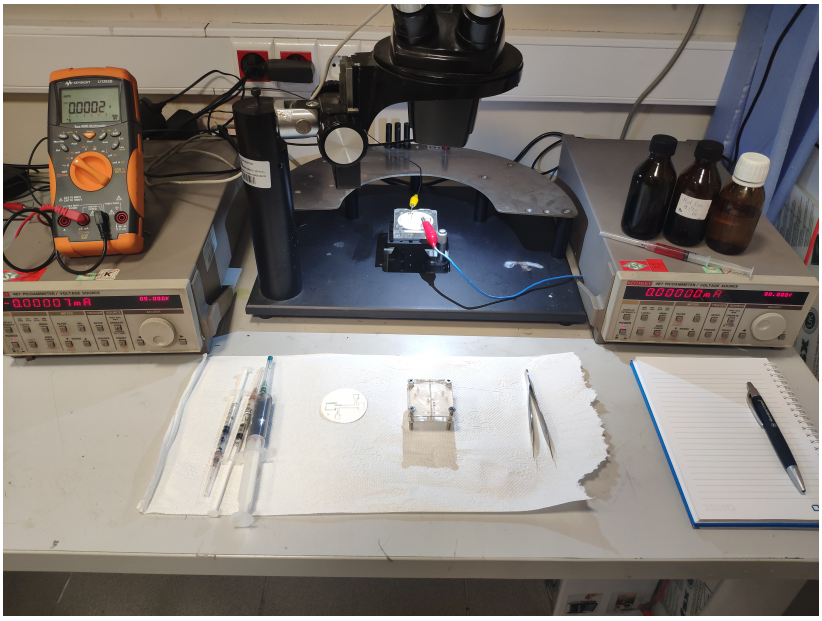

Figure 4.1. Photograph of test environment with related equipments

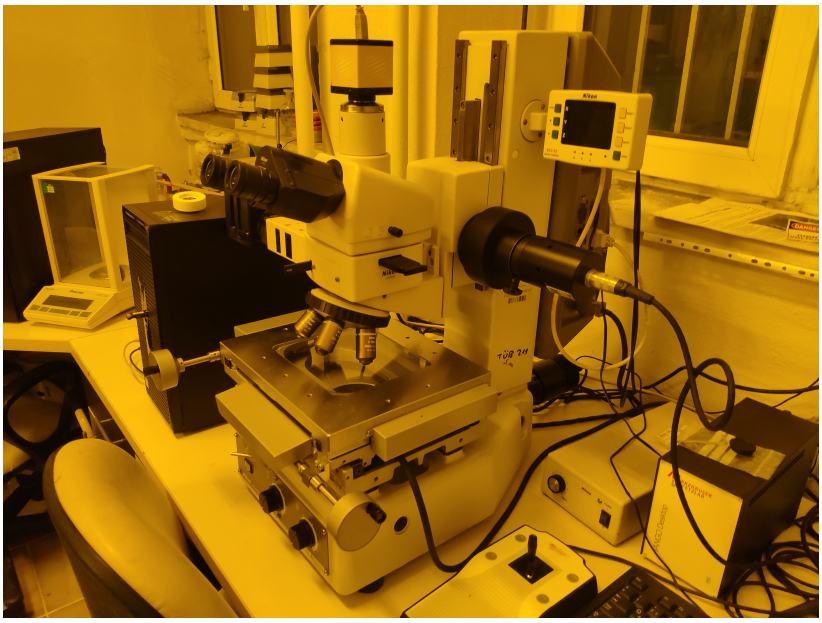

Figure 4.2. Photograph of test environment Nikon microscope.

evaluate the performance of the paper in EOP system.

As we discussed in Chapter 3, a new device was fabricated to measure pressure driven flow in Figure 4.3. Illustration of the fabricated device shows how measurements are be done. The water height of the tube was changed five times to achieve five different pressure values. The pressure value was calculated through a simple formula;

$$P = m \times g \times h \tag{4.1}$$

After changing the water height, the results are shown in Figure 4.8. It can be clearly seen in the figure that the performance was improved by 57 times in pressure driven flow on 0.2 μ membrane compared to Whatman filter paper. It is thus seen that pulling performance significantly improved and it is revealed that Whatman filter paper is not fit for our system in pulling experiments.

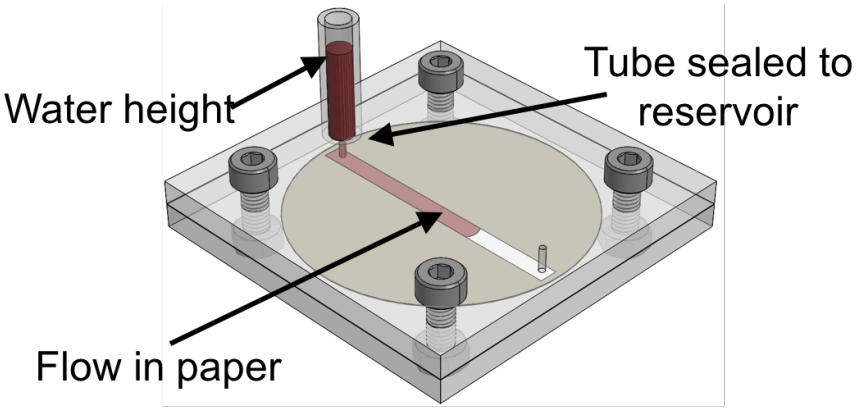

Figure 4.3. Setup to measure pressure driven flow to be used in hydraulic resistance calculation.

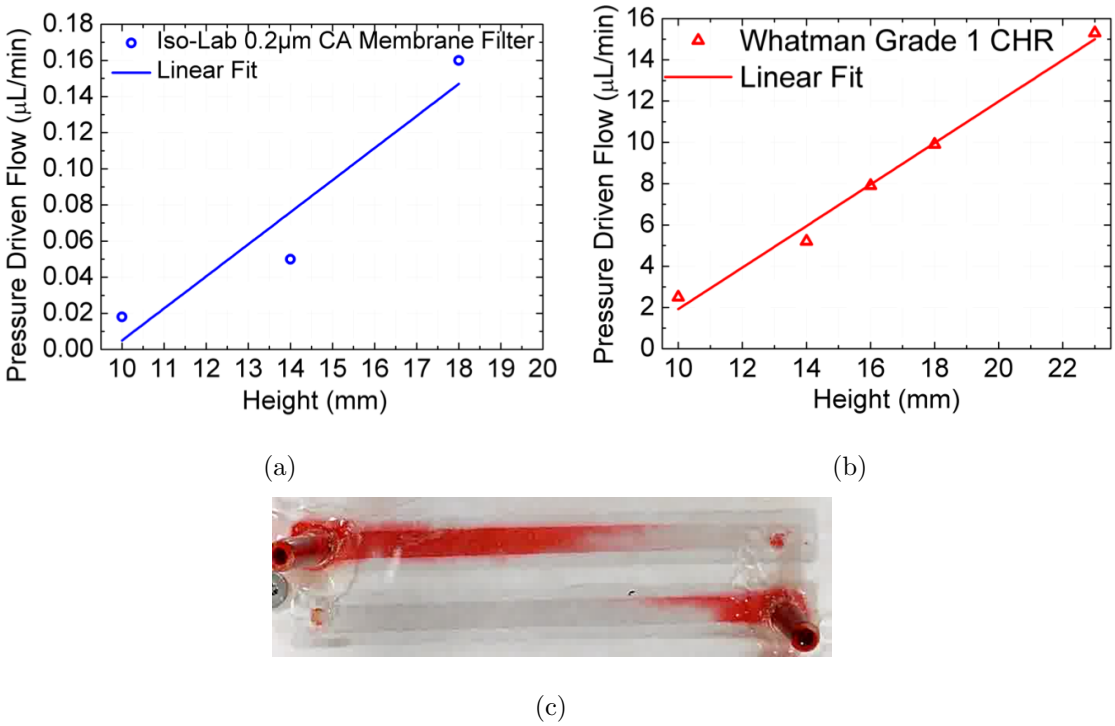

(a) (b)

(c)

Figure 4.4. Pressure driven flow results of the Whatman Grade 1 CHR filter paper (a) and 0.2 μm cellulose acetate (CA) membrane filter (b) as the applied water height changes. (c) demonstrate of experiments [1].

4.3. pH Relations

The EOP can generate high flow rates over an extended pH range of at least 2 to 12, a significant advantage over previously fabricated EOPs, which typically have a more limited range in which they can achieve high flow rates [27]. pH can play an important role to improve electro-osmotic pumping, because there would be ion changing in electrode reservoir. It can be emphasized that electrophoresis would also play an important role.

Figure 4.5 shows us pH indicator movement under electric field on the paper substrate. In section (a), paper substrate was sprinkled with pH indicator. In section (b), electric field was applied on electrode reservoir by carbon electrodes in the paper substrate. In section (c), it can be clearly seen that pH indicator began moving through the pumping channel. In section (d), pH indicator traveled across the sides of the bridges and then in section (e), pH indicator dominates paper with respect to electric field streamline that is also shown in simulation Figure2.6. While this process was taking place, there was a movement in field free region where it can be clearly seen that red dye was pumped similar to what is shown in Figure2.6. However, it can be said that these experiments are just a starting point of pH measurements, which also is in the road map of this research.

4.4. Electro Osmotic Pumping Measurements

In this part of thesis, electro-osmotic pumping measurements will be demonstrated. Measurements are based on flow within paper and microfluidic channel. Moreover, ion concentration will analyse that plays an important role as we previously discussed. The purpose of the measurement is to achieve the best pumping performance.

As we previously discussed, measurements of devices are crucial when working with the integrated system. First of all, paper based measurements were done by using the same methodologies, results of which are shown in in Figure 4.7. Here, the forward

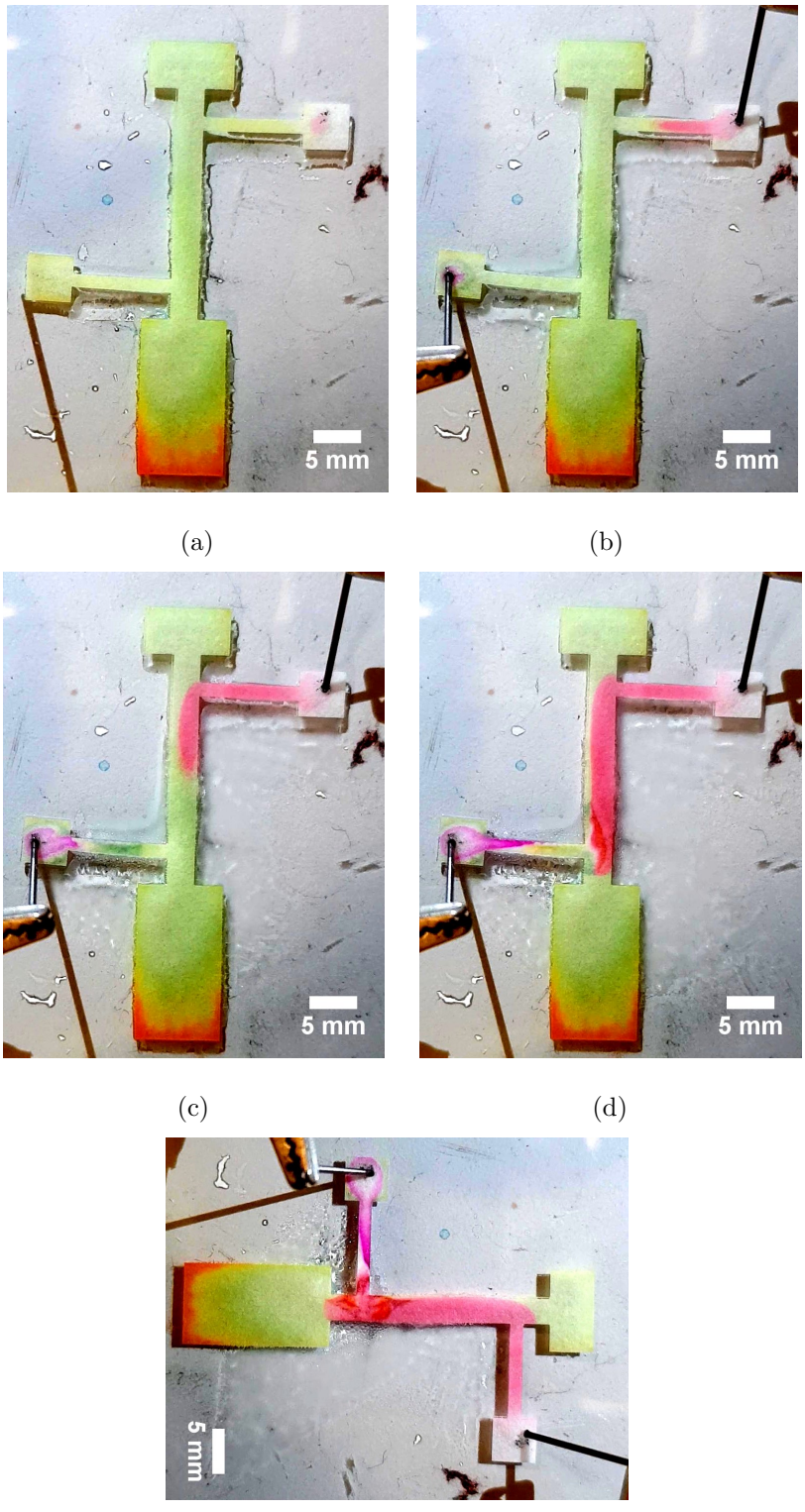

(a) (b)

(c) (d)

(e)

Figure 4.5. Demonstration of pH indicator movement in electric field.Whatman grade was wetted by pH indicator in section (a), electric field was applied in (b), indicator moved from gate to gate in (c),(d) and finally flow can be observed in main channel in section (e). [28].

liquid flow from t=0 to t=720s and reverse liquid flow from t=720s to t=1200s can be seen clearly. In this experiment, we use Whatman paper, so pressure driven flow affects slightly the movement of the liquid, on the other hand the movement of the liquid can be pulled and push mechanism, so it could be said that the total amount of pressure driven flow can be neglected. Furthermore, Figure 4.6 shows electro-osmotic pumping on the continuous microfluidic channel using membrane filter. Photos are taken (a) at the beginning, (b) at 300 seconds, (c) at 600 seconds, (d) at 900 seconds, (e) at 1200 seconds, (f) at 1500 seconds. In this demonstration, free channel chip was used, which can be seen in in Figure 3.10. EOP was performed with 8 mm water height load pressure, average electric field of 61 V/cm and the measured flow velocity is 1.4 μm/s [1].

Liquid samples with different ion concentrations were used in substrates made of three different papers. Similarly in Figure 4.6, free microfluidic channel was used and liquid movement was analysed in ImageJ. Figure 4.8 shows observation of volumetric flow when various voltages were applied with different ion concentrations in Whatman Grade, Iso-Lab Cellulose Acetate and Iso-Lab Nitrocellulose papers in (a),(b) and (c) respectively. It can be clearly seen that there is a parabolic relationship between ion concentration and volumetric flow. Best results can be observe at 100 mM, 50 mM and 10 mM in Whatman, cellulose acetate, cellulose nitrate respectively. After achieving these results, integration experiments were done in relation. After continuous and paper based channel measurements are done, integration process follows.

4.5. Integration of Electro-osmotic Pumps

Integration of EOPs are one of the most important part of this thesis. Non integrable chips do not have significant implications in real life since their capabilities are limited. EOPs can be integrated without moving parts, which puts them at the focus of a considerable research area. The main idea behind the integration in this thesis is mixing and metering, serving as proof of control mechanism. It is a fact that device limitations provide different integration scenarios. Figure 4.10 shows us the use of two optimized EOPs in mixing and metering. Red and blue fluid flows are pumped

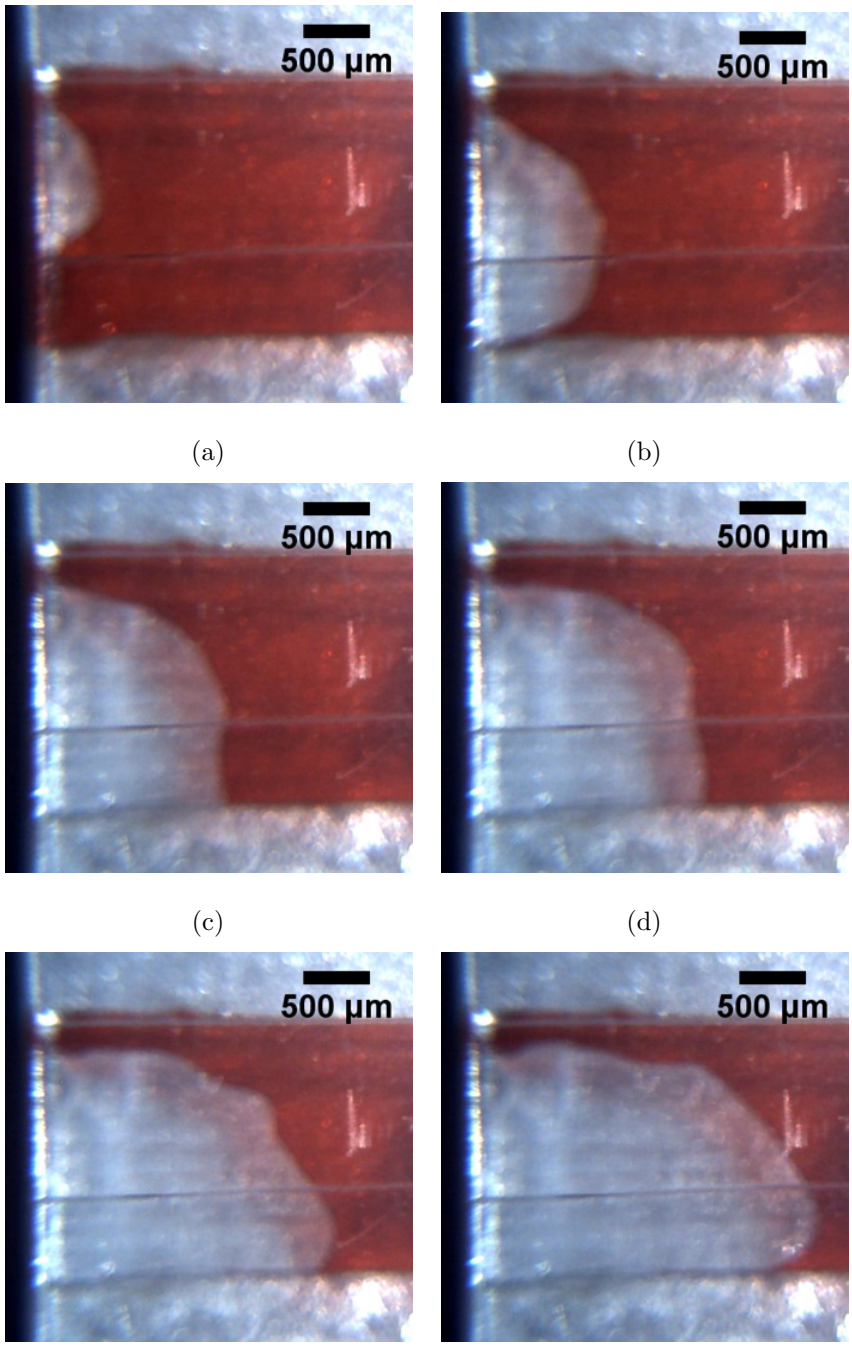

Figure 4.6. electro-osmotic pumping on the continuous microfluidic channel using membrane filter. electro-osmotic pumping on the continuous microfluidic channel using membrane filter. Photos are taken (a) at the beginning, (b) at 300 seconds, (c) at 600 seconds, (d) at 900 seconds, (e) at 1200 seconds, (f) at 1500 seconds. [1].

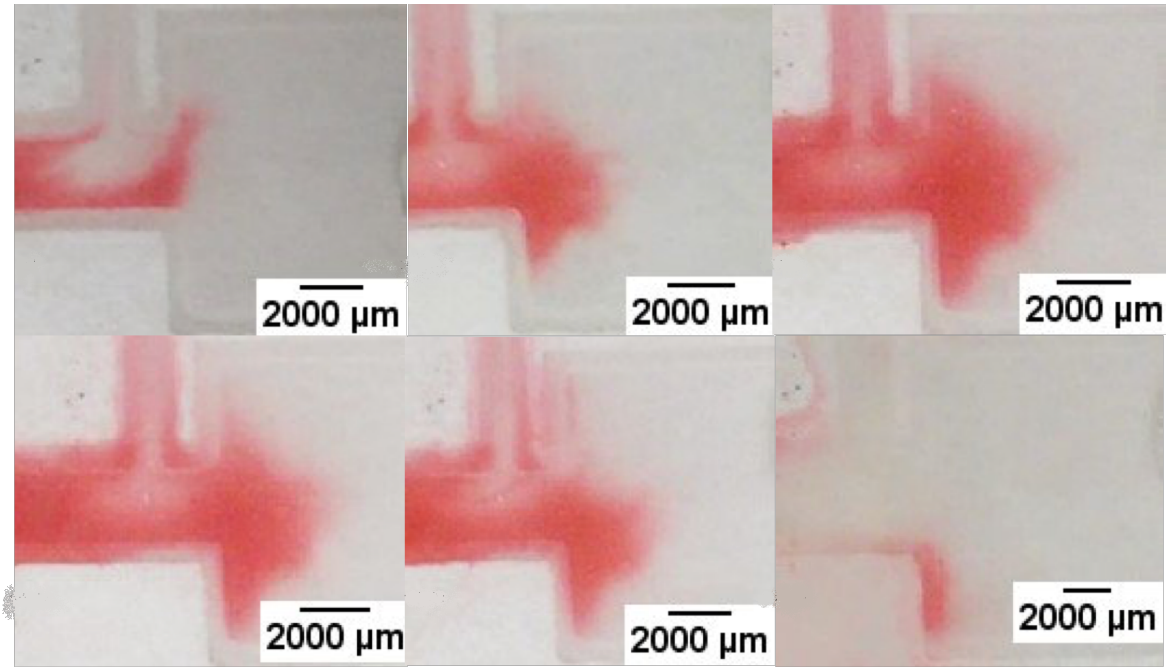

Figure 4.7. Forward liquid flow in the electric-field free main channel at t=0, t=180 s and t=720 s after +113 V/cm electric field magnitude is applied between electrode reservoirs using DI Water. Reverse liquid flow at t=840 s, t=960 s and t=1200 s after -113 V/cm is applied between electrode reservoirs starting at t=720 s. [19]

.

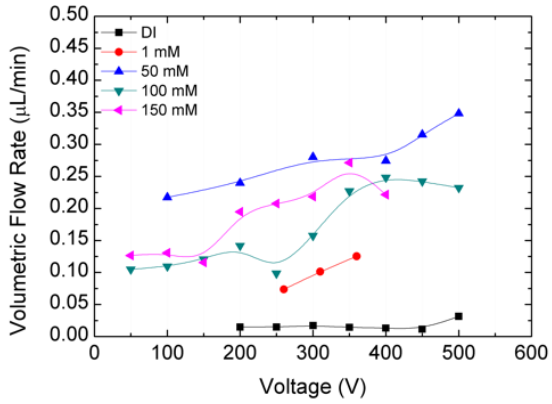

(a)

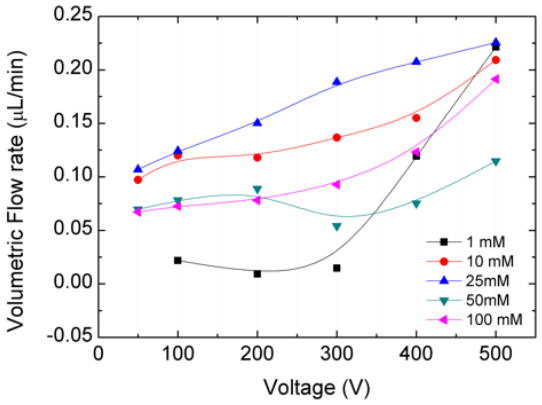

(b)

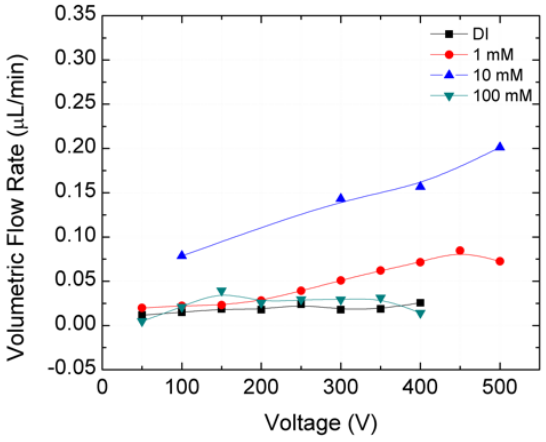

(c)

Figure 4.8. Various voltage was applied with different ion concentrations to observe volumetric flow in Whatman Grade, Iso-Lab Cellulose Acetate and Iso-Lab Nitrocellulose in (a),(b) and (c) respectively.

by two separate systems that are connected to each other via a paper channel. The main idea behind this experiment is that two EOPs can be integrated with each other and with one channel where the mixing and metering occurs. As Figure 4.10 shows, two main reservoirs have blue and red dyes separately. Electric current was applied to the system also separately. This is due to the fact that the two pumps working simultaneously constitutes a configuration in which the electric field streamlines can cancel each other out if the currents are not applied separately. In this experiment, blue dye was pumped until it reached to the field free region. Same procedure was applied the red dye as well. Next, voltage was applied at a certain interval until they reached the collector reservoir. Finally, mixing and metering can be performed in collector reservoir.

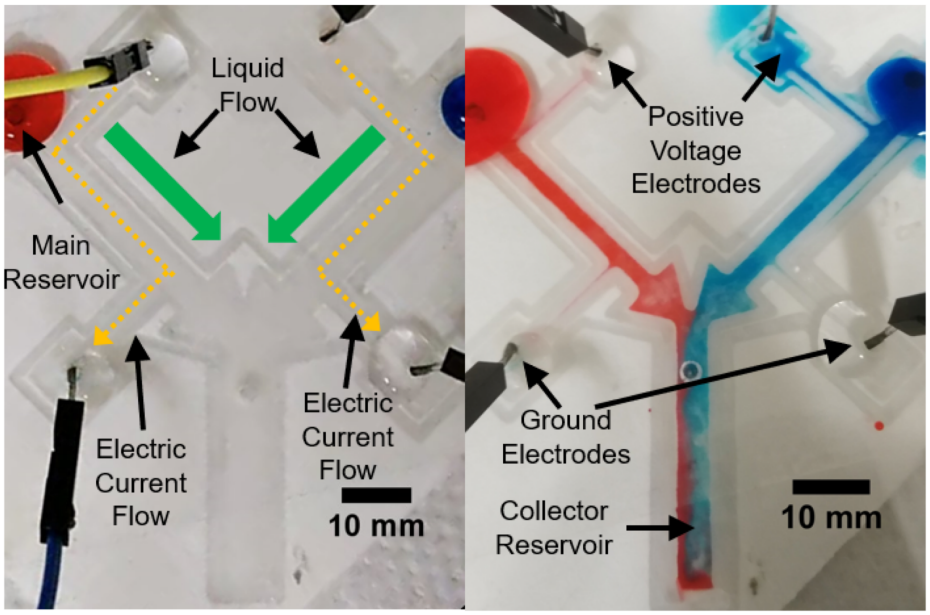

Figure 4.9. An example of a microfluidic system with two pumps using DI water. Two EOPs act together to pump two different liquids into a common channel, showing controlled liquid handling. [19].

Continuous channel integration plays an important role in this thesis as stated previously. Figure 4.10 demonstrates the controlling of two different liquids with two integrated EOPs within continuous Y-shaped microfluidic channel. Even when leakage problem can be observed it is not related to integration approach, rather it stems

from the difficulties of the fabrication process. In Figure 4.10 section (b), yellow EOP is turned on while blue EOP is turned off, clearly showing that even blue liquid has pressure driven flow, paper based porous domain will block its movement. On the other side, yellow liquid was pumped first to paper channel and then to continuous microfluidic channel. In section (c), yellow liquid passed from porous EOP to continious microfluidic channel while blue liquid is restrained, clearly showing us the presence of motion control as described previously [1].

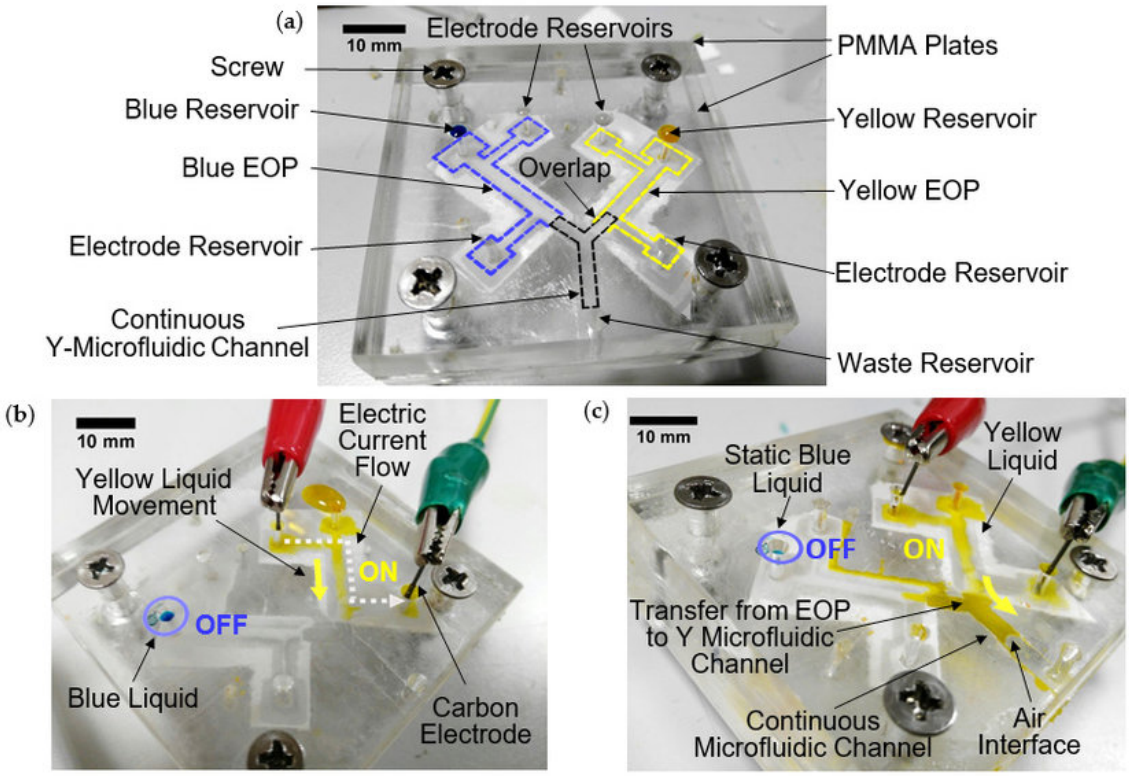

Figure 4.10. (a) Demonstration of motion control of two different liquids with two integrated EOPs and a continuous Y-shaped microfluidic channel; (b) Yellow EOP is turned on while blue EOP is turned off; (c) Yellow liquid passes from porous EOP to continuous microfluidic channel while blue liquid is restrained. [1].

As previously discussed, leakage problem and fabrication difficulties were solved by several experiments and finally integration of free channel was performed as demonstrated in Figure 4.11. CA membrane filter has powerful pulling skills because of high porosity, enabling it to pull fluid flow in free channel. The experiment has several steps to achieve final mixing and metering in the free channel. First of all, different ion con-

centrations were measured as previously discussed, and as Figure 4.8 shows us 50 mM solution has most effective EOP performance. Secondly, two EOPs were simulated in COMSOL to achieve best pumping performance. Previously, 120° angle difference was used in paper channel integration in Figure 4.10. On the other hand, 120° design was used for better pulling performance in free channel because of fabrication facilitation. Last but not least, two EOPs worked separately, because while two pumps are working together, they affected each other via electric field movement, which can be observed in the free channel transaction. Figure 4.11 clearly demonstrates that the system has air interface that eliminates pressure driven flow, where in section (c), flow was created PDF, can escape on air interface. Working principle is almost the same with respect to applying voltage, finally in section (g), mixing can be observed in continuous microfluidic channel by enabling two EOPs.

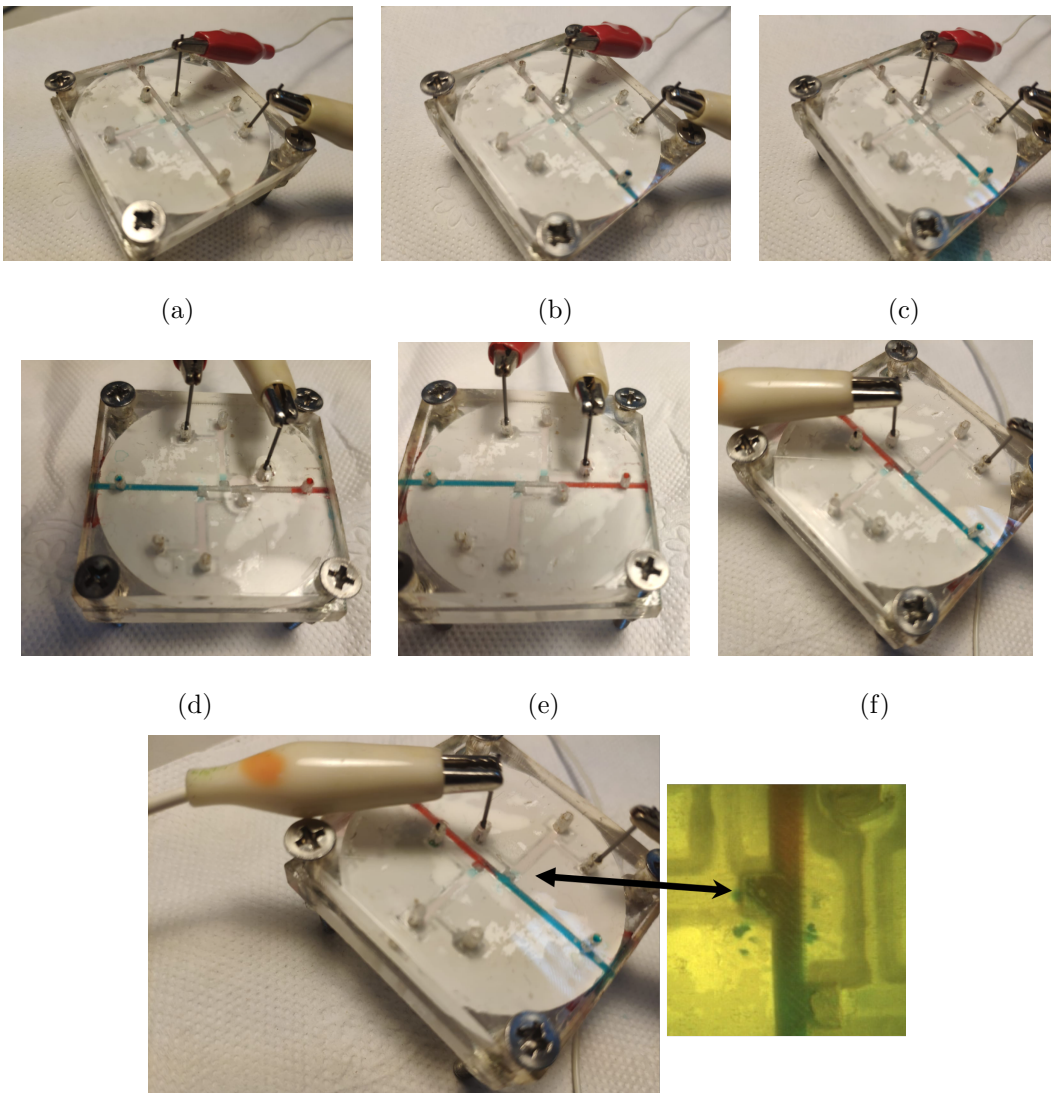

(a) (b) (c)

(d) (e) (f)

(g)

Figure 4.11. (a),(b),(c) Demonstration of motion control of two different liquids with two integrated EOPs and a continuous microfluidic channel.(d),(e),(f)demonstrate blue dye passes from porous EOP to continuous microfluidic channel while red dye passes also.(g) shows mixing and metering of red and blue liquid

5. CONCLUSIONS AND FUTURE WORK

In this thesis, a paper based integrated microfluidic system using EOPs with liquid bridges are designed, simulated, optimized, fabricated and integrated. After several fails of experiments, standard of design and fabrications became considerably refined in order to improve system performance compared to starting the day of research. In conclusion chapter, research and studies will be demonstrated and the previous studies and chapters are concluded, and then the results are evaluated. Since, there is no perfect research and there is always need for more improvements. Therefore the possibilities regarding future work are also presented.

As previously discussed in the first chapter, paper based integrated microfluidic system using EOPs with liquid bridges is the main aim. Theory behind EOPs was revealed and the positive impact of this unique method especially in paper based applications are mentioned. Moreover, potential and capabilities of integration are one of the most important part of this thesis. Even though the system works properly, it is the practical application and integration that makes it valuable.

In Chapter 2, theory and system description are given. The concept of EOPs, and research background shows us there is a great potential since the system is well-suited for implementation and it contains no moving part. Moreover, the parameters of design show us different models and designs alternatives can be created depending on the system. Simulations are performed using COMSOL Multiphysics to optimize systems. There are several parameters that affected performance of EOPs and they are simulated through parametric sweep method. Moreover, multiphysics made it possible the solving of related equations together and the finite element modeling, allowing for better optimization process.

In Chapter 3, different fabrication processes were demonstrated. To begin with, silicone melting is the first fabrication method that was tried, but there are some limitations and obstacles related to it. Laser cutting can fail at fabrication reliability.

It can also sometimes damage the paper. When it comes to melting silicone, wetting of paper is one of the most challenging parts, which can take sometimes an hour. In contrast, wax printing is easy to create features. It also has some limitations regarding the printing of small features. Last but not least, laser micromachining is the most useful tool that is tried to create microfluidic channels. One of the most challenging steps is that the characterization should be done for every single poly-carbonate plate.

In Chapter 4, characterization and measurement devices were described. Characterization of EOPs is one of the most important phenomena that makes it possible to understand integration capabilities. Several experiments were done to realize potential and obtain practical results. Paper based channel measurements and characterization are done based on paper type. It was observed that porosity played an important role at that point. Later on, continuous microfluidic channel was seen to be crucial in implementation of other systems. It was seen that 113 V/cm electric field creates 50 μm/s electro-osmotic velocity with DI water and 70 μA electrical current creates 1 L/min volumetric flow rate with 2 mM NaCl solution in paper based channel. Moreover, continuous channel of paper based EOPs was implemented for the first time. 30 nL volumetric flow rate was achieved by 82 V/cm electric field when using 50 mM NaCl as the solution. Integration of EOPs was demonstrated in two different experiments that demonstrate motion control and mixing and metering in continuous channel.

Future work is based on improvement of EOPs. Analyzing paper porosity structure is one the most important topics. Based on calculations, x, y, and z direction porosity measurements are necessary to understand better the operation principle of EOPs. Control mechanism is one of the key factors that should be optimized and characterized in the future so that the capabilities of pumping skills can be understood better. Analysis of the pH mechanism is also important in order to have a better grasp and analysis of the theory of electrophoresis and electro-osmosis. This research step can also can be divided into two domains with different integration capabilities. Furthermore, integration of multiple EOPs is very critical to create complex system that will further the research area. Last but not least, a solution for the wetting problem, which was faced several times, should be investigated in order to minimze time losses.

REFERENCES

1. Kaya, K., A. Y. Celik and S. Mutlu, "Integration of Paper Based Electro-Osmotic Pumps to Continuous Microfluidic Channels", *Multidisciplinary Digital Publishing Institute Proceedings*, Vol. 2, p. 870, 2018.

2. Dittrich, P. S. and A. Manz, "Lab-on-a-chip: microfluidics in drug discovery", *Nature reviews Drug discovery*, Vol. 5, No. 3, p. 210, 2006.

3. Whitesides, G. M., "Cool, or simple and cheap? Why not both?", *Lab on a Chip*, Vol. 13, No. 1, pp. 11–13, 2013.

4. Martinez, A. W., S. T. Phillips, B. J. Wiley, M. Gupta and G. M. Whitesides, "FLASH: a rapid method for prototyping paper-based microfluidic devices", *Lab on a Chip*, Vol. 8, No. 12, pp. 2146–2150, 2008.

5. Dey, R., S. Kar, S. Joshi, T. K. Maiti and S. Chakraborty, "Ultra-low-cost 'paper-and-pencil'device for electrically controlled micromixing of analytes", *Microfluidics and Nanofluidics*, Vol. 19, No. 2, pp. 375–383, 2015.

6. Zeng, S., C.-H. Chen, J. C. Mikkelsen Jr and J. G. Santiago, "Fabrication and characterization of electroosmotic micropumps", *Sensors and Actuators B: Chemical*, Vol. 79, No. 2-3, pp. 107–114, 2001.

7. Maier, R. S., E. Nybo, J. D. Seymour and S. L. Codd, "Electroosmotic flow and dispersion in open and closed porous media", *Transport in Porous Media*, Vol. 113, No. 1, pp. 67–89, 2016.

8. Gao, M. and L. Gui, "A handy liquid metal based electroosmotic flow pump", *Lab on a Chip*, Vol. 14, No. 11, pp. 1866–1872, 2014.

9. Mutlu, S., C. Yu, P. Selvaganapathy, F. Svec, C. H. Mastrangelo and J. M. Frechet,

"Micromachined porous polymer for bubble free electro-osmotic pump", *Technical Digest. MEMS 2002 IEEE International Conference. Fifteenth IEEE International Conference on Micro Electro Mechanical Systems (Cat. No. 02CH37266)*, pp. 19–23, IEEE, 2002.

10. Muthu, S., F. Svec, C. H. Mastrangelo, J. M. Fréchet and Y. B. Gianchandani, "Enhanced electro-osmotic pumping with liquid bridge and field effect flow rectification", *17th IEEE International Conference on Micro Electro Mechanical Systems. Maastricht MEMS 2004 Technical Digest*, pp. 850–853, IEEE, 2004.

11. Mandal, P., R. Dey and S. Chakraborty, "Electrokinetics with "paper-and-pencil" devices", *Lab on a Chip*, Vol. 12, No. 20, pp. 4026–4028, 2012.

12. Reuss, F. F., "On a new effect of galvanic ee electricity", *Mem. Soc. Imp. Natur. Moscow*, Vol. 2.

13. Wang, X., C. Cheng, S. Wang and S. Liu, "Electroosmotic pumps and their applications in microfluidic systems", *Microfluidics and Nanofluidics*, Vol. 6, No. 2, pp. 145–162, 2009.

14. Brask, A., G. Goranović and H. Bruus, "Theoretical analysis of the low-voltage cascade electro-osmotic pump", *Sensors and Actuators B: Chemical*, Vol. 92, No. 1-2, pp. 127–132, 2003.

15. Nguyen, N. T. and S. T. Wereley, "Fundamentals and Applications of Microfluidics, Artech House", *Inc., Norwood, MA*, pp. 292–337, 2002.

16. Hrdlicka, J., P. Cervenka and D. Snita, "Mathematical modeling of traveling-wave electroosmotic micropumps by using of the Weak Form", *continuity*, Vol. 4, p. 0.

17. Tandon, V., S. K. Bhagavatula, W. C. Nelson and B. J. Kirby, "Zeta potential and electroosmotic mobility in microfluidic devices fabricated from hydrophobic polymers: 1. The origins of charge", *Electrophoresis*, Vol. 29, No. 5, pp. 1092–1101,

2008.

18. Durlofsky, L. and J. Brady, "Analysis of the Brinkman equation as a model for flow in porous media", *The Physics of fluids*, Vol. 30, No. 11, pp. 3329–3341, 1987.

19. Celik, A. Y., K. Kaya and S. Mutlu, "Paper based integrated microfluidic system using electro-osmotic pumps with liquid bridges", *2018 IEEE Micro Electro Mechanical Systems (MEMS)*, pp. 1225–1228, IEEE, 2018.

20. Gong, X., X. Yi, K. Xiao, S. Li, R. Kodzius, J. Qin and W. Wen, "Wax-bonding 3D microfluidic chips", *Lab on a Chip*, Vol. 10, No. 19, pp. 2622–2627, 2010.

21. Rajaram, N., J. Sheikh-Ahmad and S. Cheraghi, "CO2 laser cut quality of 4130 steel", *International Journal of Machine Tools and Manufacture*, Vol. 43, No. 4, pp. 351–358, 2003.

22. Carrilho, E., A. W. Martinez and G. M. Whitesides, "Understanding wax printing: a simple micropatterning process for paper-based microfluidics", *Analytical chemistry*, Vol. 81, No. 16, pp. 7091–7095, 2009.

23. Lu, Y., W. Shi, L. Jiang, J. Qin and B. Lin, "Rapid prototyping of paper-based microfluidics with wax for low-cost, portable bioassay", *Electrophoresis*, Vol. 30, No. 9, pp. 1497–1500, 2009.

24. Gower, M. C., "Industrial applications of laser micromachining", *Optics Express*, Vol. 7, No. 2, pp. 56–67, 2000.

25. Cheng, J.-Y., C.-W. Wei, K.-H. Hsu and T.-H. Young, "Direct-write laser micromachining and universal surface modification of PMMA for device development", *Sensors and Actuators B: Chemical*, Vol. 99, No. 1, pp. 186–196, 2004.

26. Schindelin, J., I. Arganda-Carreras, E. Frise, V. Kaynig, M. Longair, T. Pietzsch, S. Preibisch, C. Rueden, S. Saalfeld, B. Schmid *et al.*, "Fiji: an open-source plat-

form for biological-image analysis", *Nature methods*, Vol. 9, No. 7, p. 676, 2012.

27. Razunguzwa, T. T. and A. T. Timperman, "Fabrication and characterization of a fritless microfabricated electroosmotic pump with reduced pH dependence", *Analytical chemistry*, Vol. 76, No. 5, pp. 1336–1341, 2004.

28. Kaya, K., "Paper based integrated microfluidic system using electro-osmotic pumps with liquid bridges", *Microfluidic Chip Design Based on Paper Based Electro-osmotic Pumps*, pp. 1–8, Boğaziçi University Senior Project, 2019.